2011 NSF-CMACS Workshop on Atrial Fibrillation (5th day)

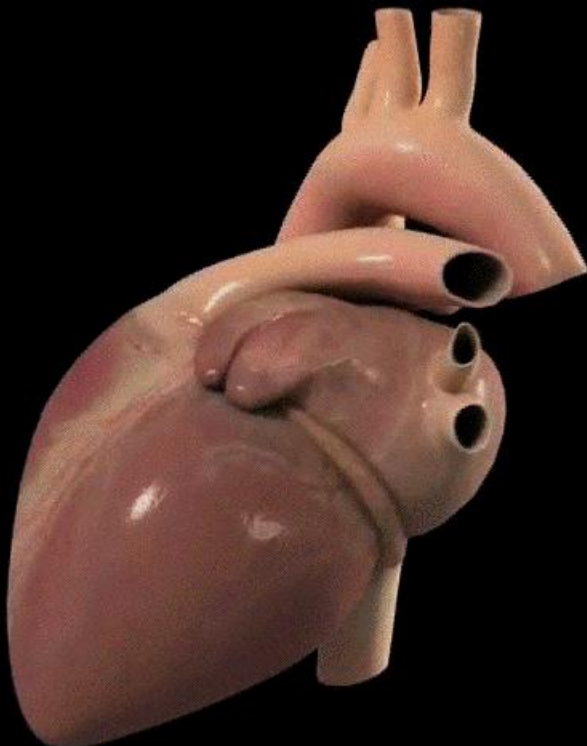

Flavio H. Fenton

Department of Biomedical Sciences
College of Veterinary Medicine,
Cornell University, NY
and
Max Planck Institute for Dynamics and
Self-organization, Goettingen, Germany

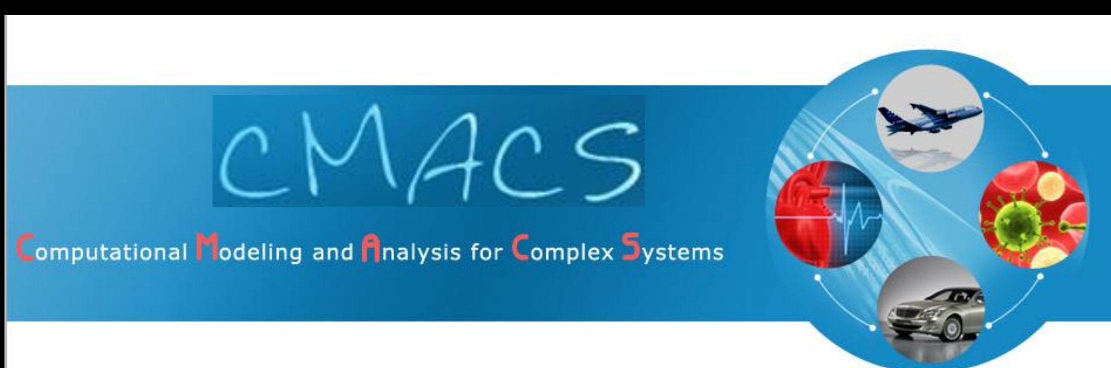

Lehman College,
Bronx, NY. Jan 3-7, 2011

3V Cell Model Equations

The model consists of 3 variables: the membrane voltage **V**, a fast ionic gate **v**, and a slow ionic gate **w**.

$$
\begin{aligned}
I_{fi}(V;\mathbf{v}) &= -\mathbf{v}\, p\,(V - V_c)(V - V_m)/\tau_d \\
I_{so}(V) &= (V - V_o)\,(1-p)/\tau_o + p/\tau_r \\
I_{si}(V;\mathbf{w}) &= -\mathbf{w}\,\left(1 + \tanh\left[k\,(V - V_c^{si})\right]\right)/(2\tau_{si})
\end{aligned}
$$

$$
\begin{aligned}
\frac{\partial V}{\partial t} &= \frac{\partial^2 V}{\partial x^2} + (a - V)(V-1)V - v \\
\frac{\partial v}{\partial t} &= \epsilon(\beta V - \gamma v - \delta)
\end{aligned}
$$

The equations for the 3 variables are:

$$
\begin{aligned}
\partial_t V(\vec{x}, t) &= \nabla \cdot (\tilde{D}\nabla V) - I_{\text{ion}} \\
\partial_t \mathbf{v}(t) &= (1-p)\,(1-\mathbf{v})/\tau_{\mathbf{v}}^{-}(V) - p\,\mathbf{v}/\tau_{\mathbf{v}}^{+} \\
\partial_t \mathbf{w}(t) &= (1-p)\,(1-\mathbf{w})/\tau_{\mathbf{w}}^{-} - p\,\mathbf{w}/\tau_{\mathbf{w}}^{+}
\end{aligned}
$$

where $\tau_{\mathbf{v}}^{-}(V) = (1-q)\,\tau_{\mathbf{v}1}^{-} + q\,\tau_{\mathbf{v}2}^{-}$

$$
p = \begin{cases} 1 & \text{if } V \geq V_c \\ 0 & \text{if } V < V_c \end{cases} \quad \text{and} \quad q = \begin{cases} 1 & \text{if } V \geq V_{\mathbf{v}} \\ 0 & \text{if } V < V_{\mathbf{v}} \end{cases}
$$

3V Cell Model Equations

The equations for the 3 variables are:

$$
\begin{aligned}
\partial_t V(\vec{x}, t) &= \nabla \cdot (\tilde{D} \nabla V) - I_{\mathrm{ion}} \\
\partial_t \mathbf{v}(t) &= (1-p)\,(1-\mathbf{v})/\tau_{\mathbf{v}}^{-}(V) \;-\; p\,\mathbf{v}/\tau_{\mathbf{v}}^{+} \\
\partial_t \mathbf{w}(t) &= (1-p)\,(1-\mathbf{w})/\tau_{\mathbf{w}}^{-} \;-\; p\,\mathbf{w}/\tau_{\mathbf{w}}^{+}
\end{aligned}
$$

where $\tau_{\mathbf{v}}^{-}(V) = (1-q)\,\tau_{\mathbf{v}1}^{-} + q\,\tau_{\mathbf{v}2}^{-}$

$p = \begin{cases} 1 & \text{if } V \geq V_c \\ 0 & \text{if } V < V_c \end{cases}$ and $q = \begin{cases} 1 & \text{if } V \geq V_{\mathbf{v}} \\ 0 & \text{if } V < V_{\mathbf{v}} \end{cases}$

$$
\begin{aligned}
I_{fi}(V;\mathbf{v}) &= -\mathbf{v}\,p\,(V - V_c)(V - V_m)/\tau_d \\
I_{so}(V) &= (V - V_o)\,(1-p)/\tau_o + p/\tau_r \\
I_{si}(V;\mathbf{w}) &= -\mathbf{w}\;\left(1 + \tanh\left[k\,(V - V_c^{si})\right]\right)/(2\tau_{si})
\end{aligned}
$$

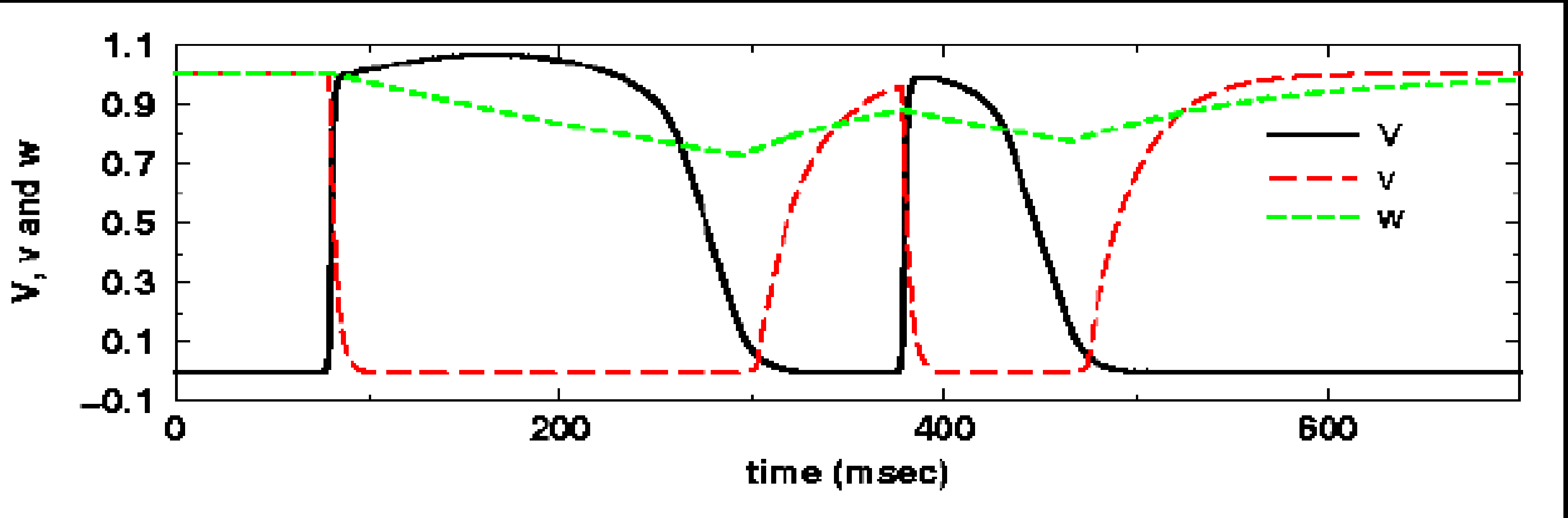

http://thevirtualheart.org/java/fk1d.html

Alternans as an example for the transition between one and multiple spiral waves

Rate Adaptation and APD Restitution

- Plotting APD as a function of the preceding DI gives what is called the restitution curve, which provides a first approximation of the system's dynamics. T=APD +DI
- APD restitution as a 1D map: $APD_{n+1} = F(DI) = F(T\text{-}APD_n)$.
- Linearizing around the fixed point $APD^* = F(DI^*)$, letting $APD_n = APD^* + \delta APD_n$, one obtains $\delta APD_{n+1} = -F'(DI)\, \delta APD_n$
- Bifurcation at $|F'(DI)| = 1$.

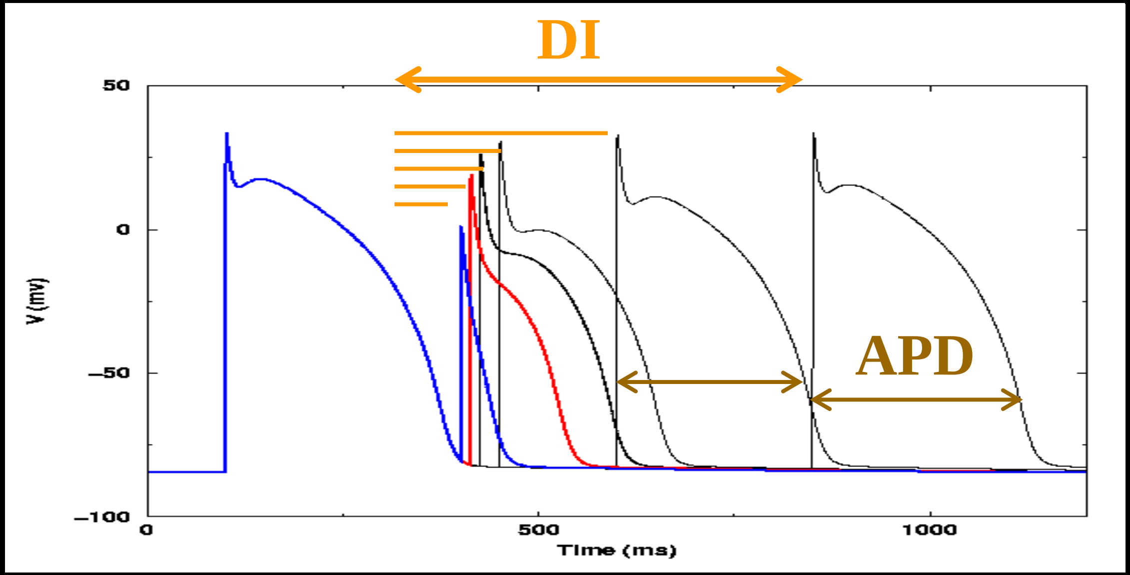

APD Restitution Curve

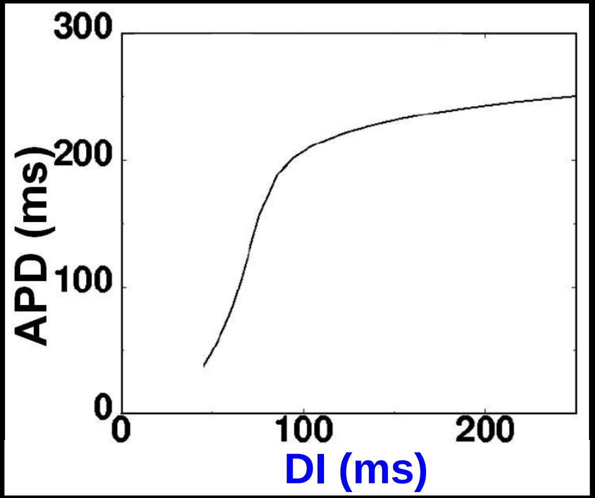

Guevara MR, Ward, Shrier, Glass L: Electrical alternans and period doubling bifurcations. Comput Cardiol 1984;167-170.

Rate Adaptation and APD Restitution

- Plotting APD as a function of the preceding DI gives what is called the restitution curve, which provides a first approximation of the system's dynamics. T=APD +DI
- APD restitution as a 1D map: $APD_{n+1} = F(DI) = F(T\text{-}APD_n)$.
- Linearizing around the fixed point $APD^* = F(DI^*)$, letting $APD_n = APD^* + \delta APD_n$, one obtains $\delta APD_{n+1} = -F'(DI)\, \delta APD_n$
- Bifurcation at $|F'(DI)| = 1$.

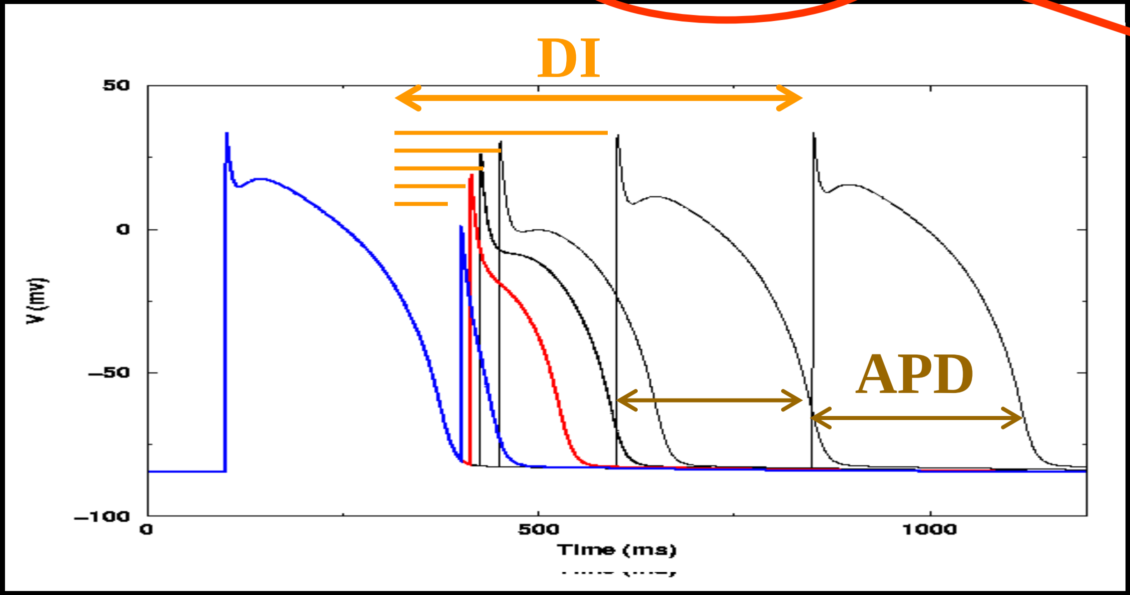

Only a first-order approximation

$F'(DI, APD, T, CV, \xi, Ca^{2+})$

Watanabe M, Fenton F. et al . JCE . 2001; 12: 196-206
Cherry EM, Fenton FH, Am J Physiol 2004; 286, H2332
Tolkacheva EG, et al., Phys Rev E 2003; 67, 031904
Cytrynbaum E, Keener JP, Chaos 2002; 12, 788

Logistic Map Dynamics: Similar to APD Restitution Dynamics

http://thevirtualheart.org/java/logisticmap.html

Period- doubling bifurcation

APD Restitution Curve

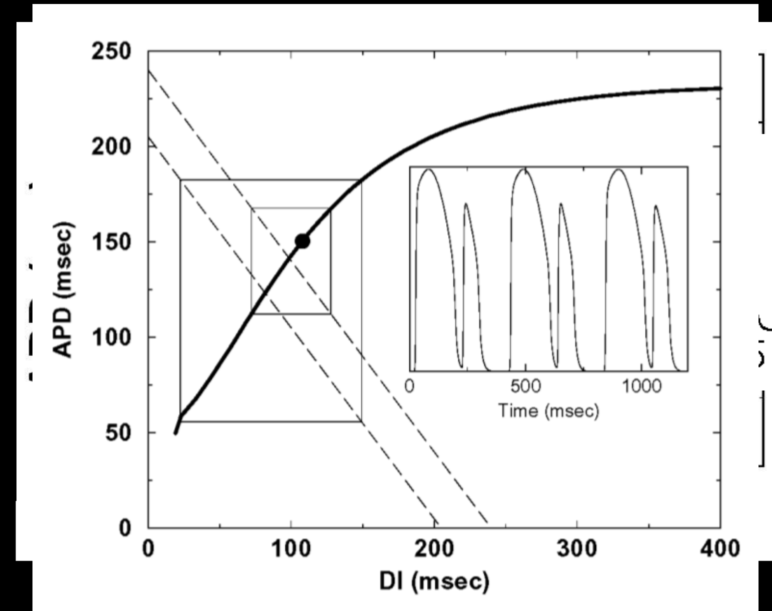

T=APD+DI

http://thevirtualheart.org/java/Hopf2a.html

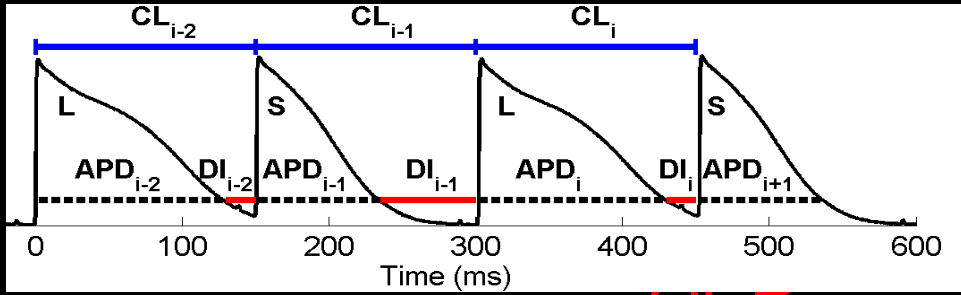

Nolasco JB, Dahlen RW: A graphic method for the study of alternation in cardiac action potentials. J Appl Physiol 1968;25:191-196.

Conduction Velocity Restitution

For a moving pulse CV changes also as a function of DI

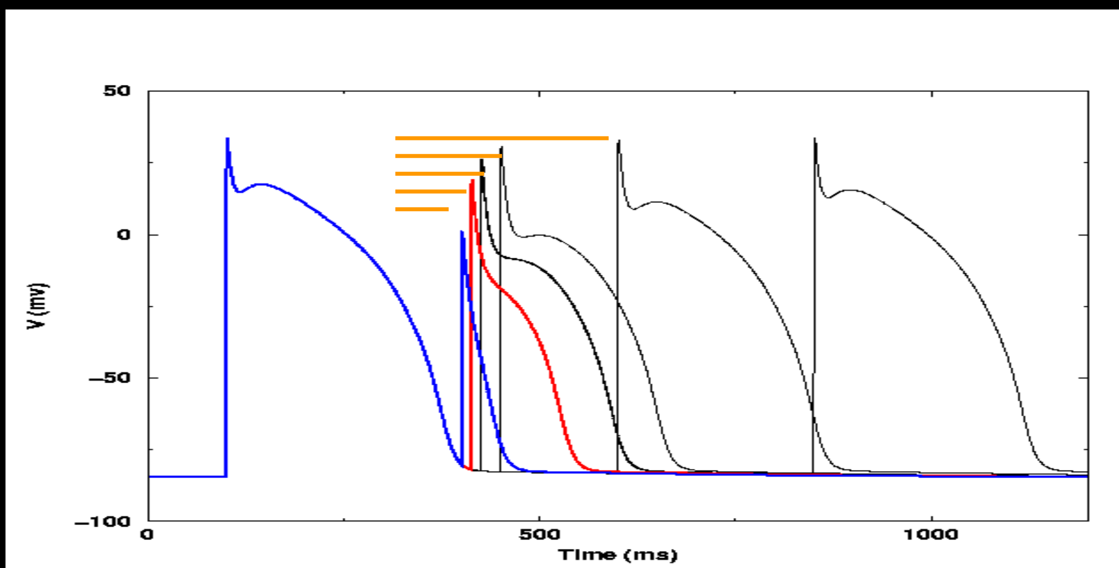

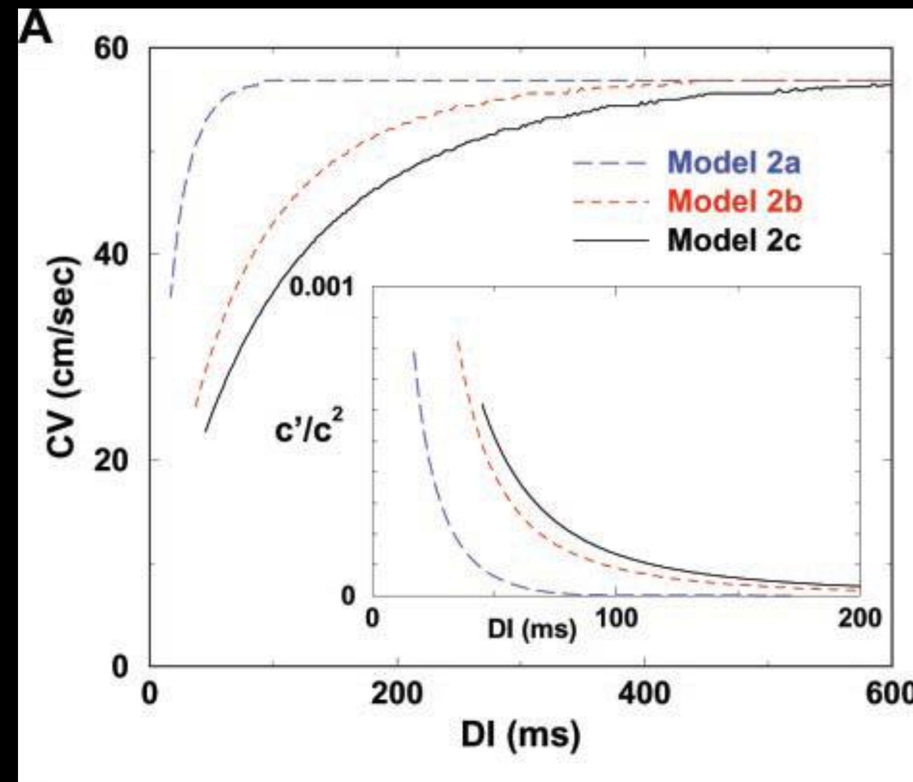

Why is alternans important?

Alternans in 1D

http://thevirtualheart.org/java/alternansmall.html

Concordant vs. Discordant Alternans

- In tissue, alternans can be either concordant or discordant.

Concordant Alternans

Discordant Alternans

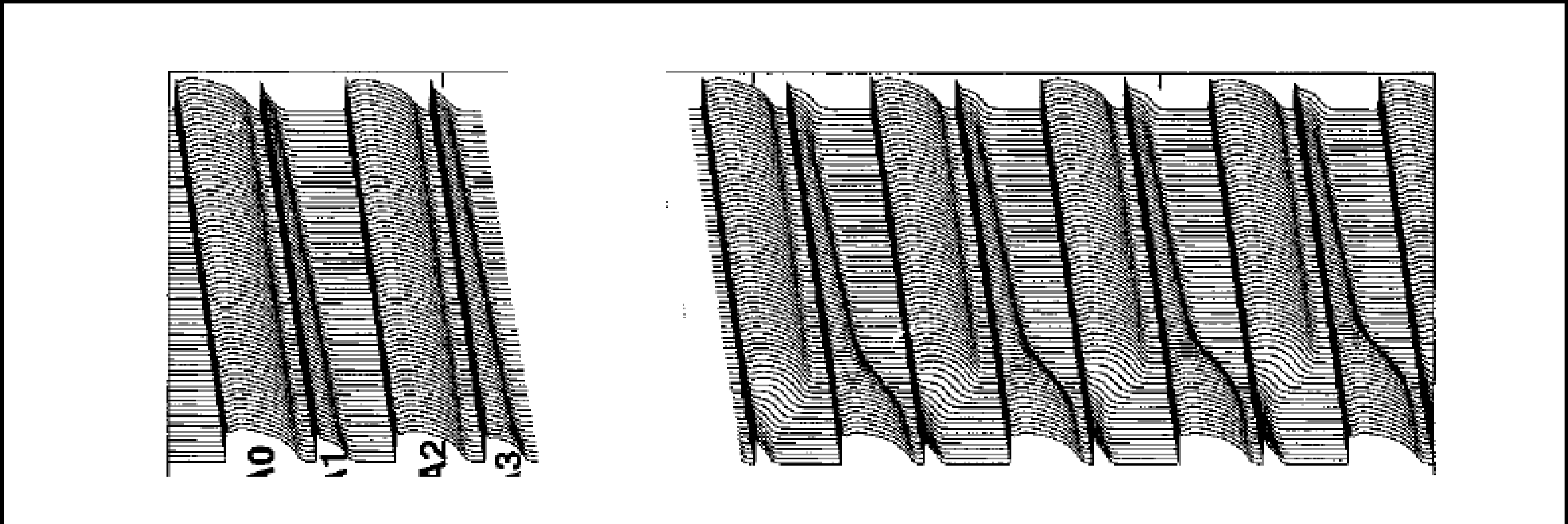

M Watanabe, FH Fenton et al. J Cardiovasc Electrophysiol 12: 196 (2001).

Discordant Alternans always develops in a ring

Can lead to very complicated dynamics

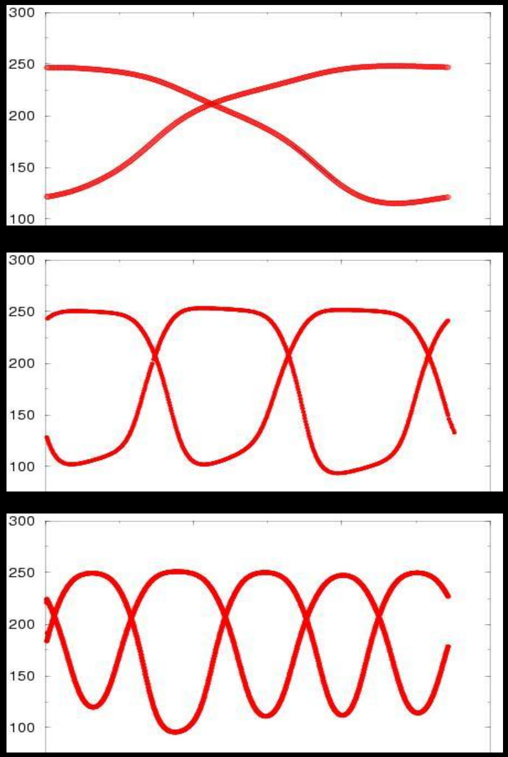

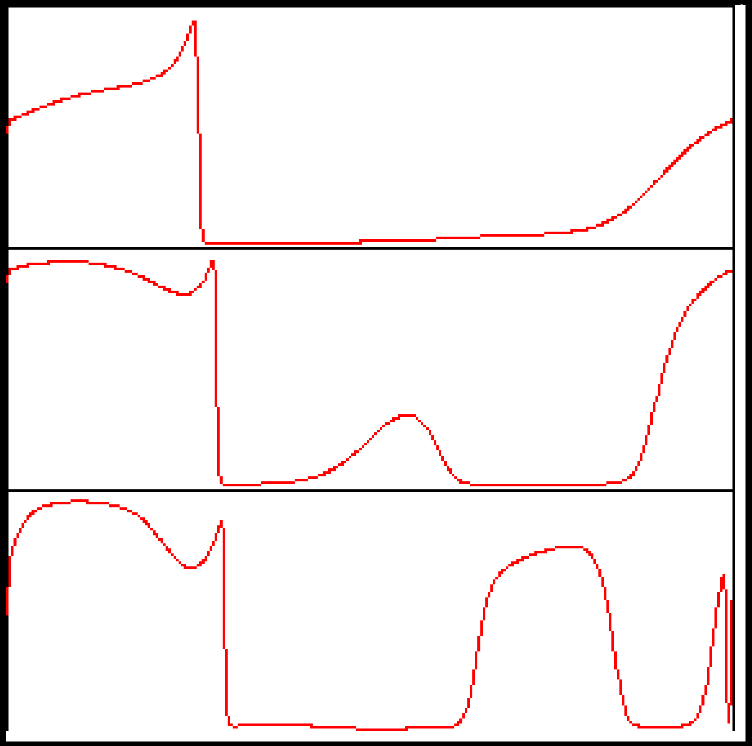

M Watanabe, FH Fenton et al. J Cardiovasc Electrophysiol 12: 196 (2001).

Alternans is Pro-arrhythmic

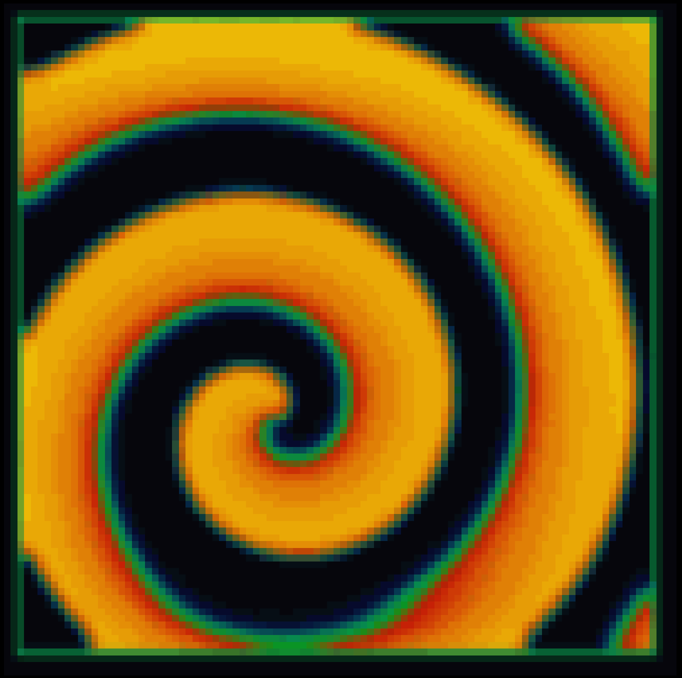

Example of breakup in 2D

We can use control algorithms to suppress alternans.
(bring the system to the unstable steady state)

1D and 2D examples

Purkinje fibers are an excellent 1d system to study.

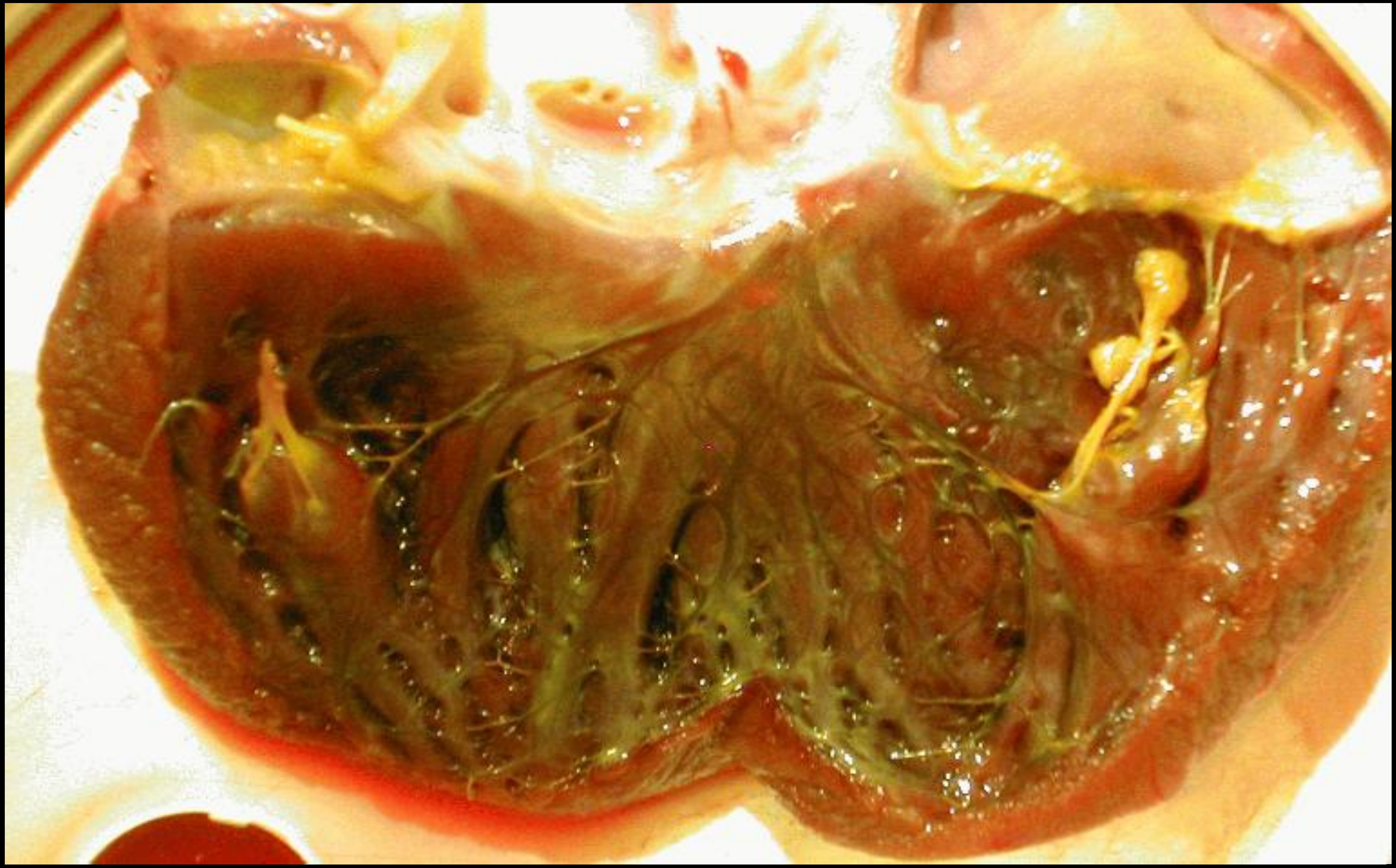

El uso de fibras de Purkinje para el estudio de alternacion

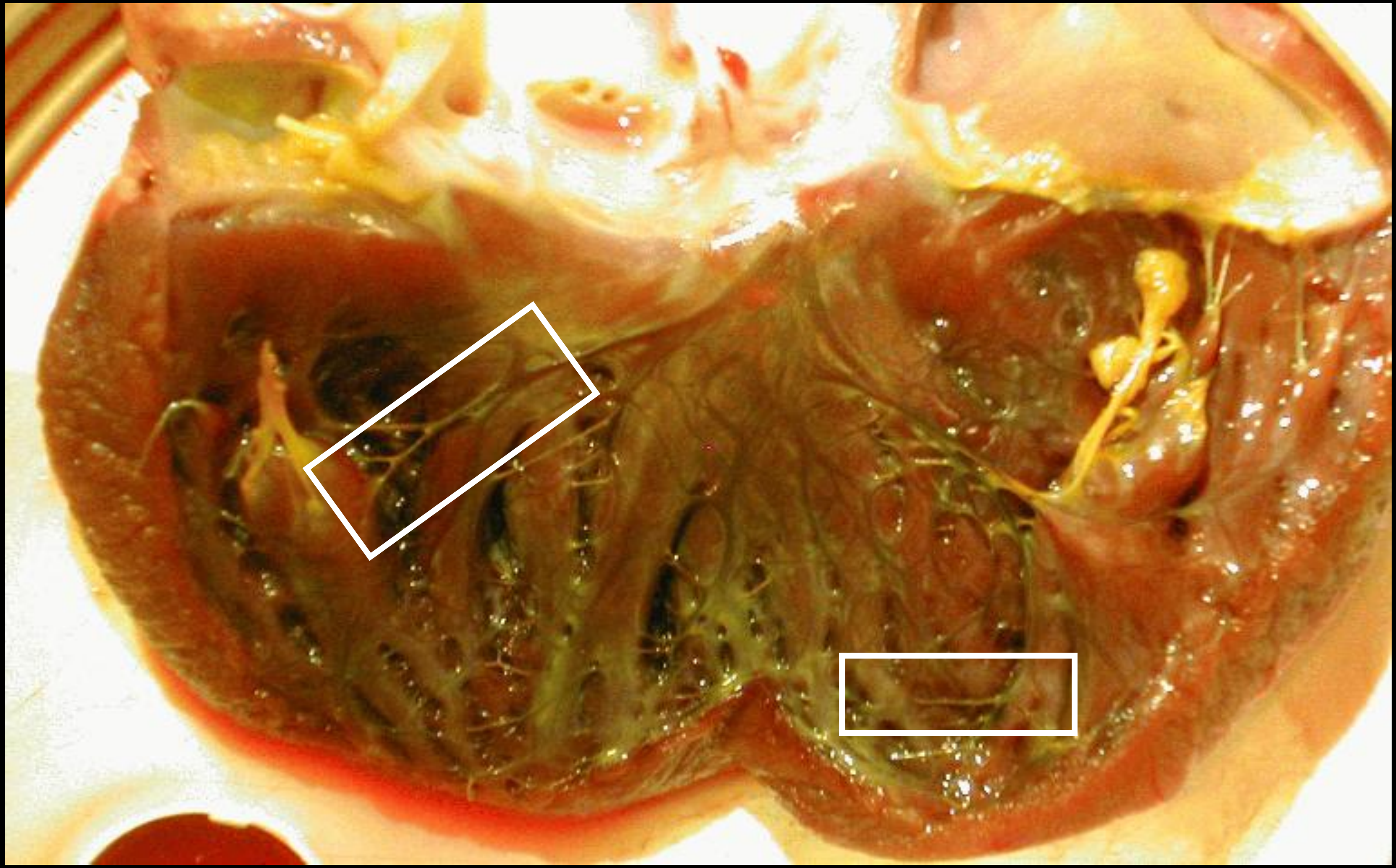

Using Purkinje Fibers to Study Alternans

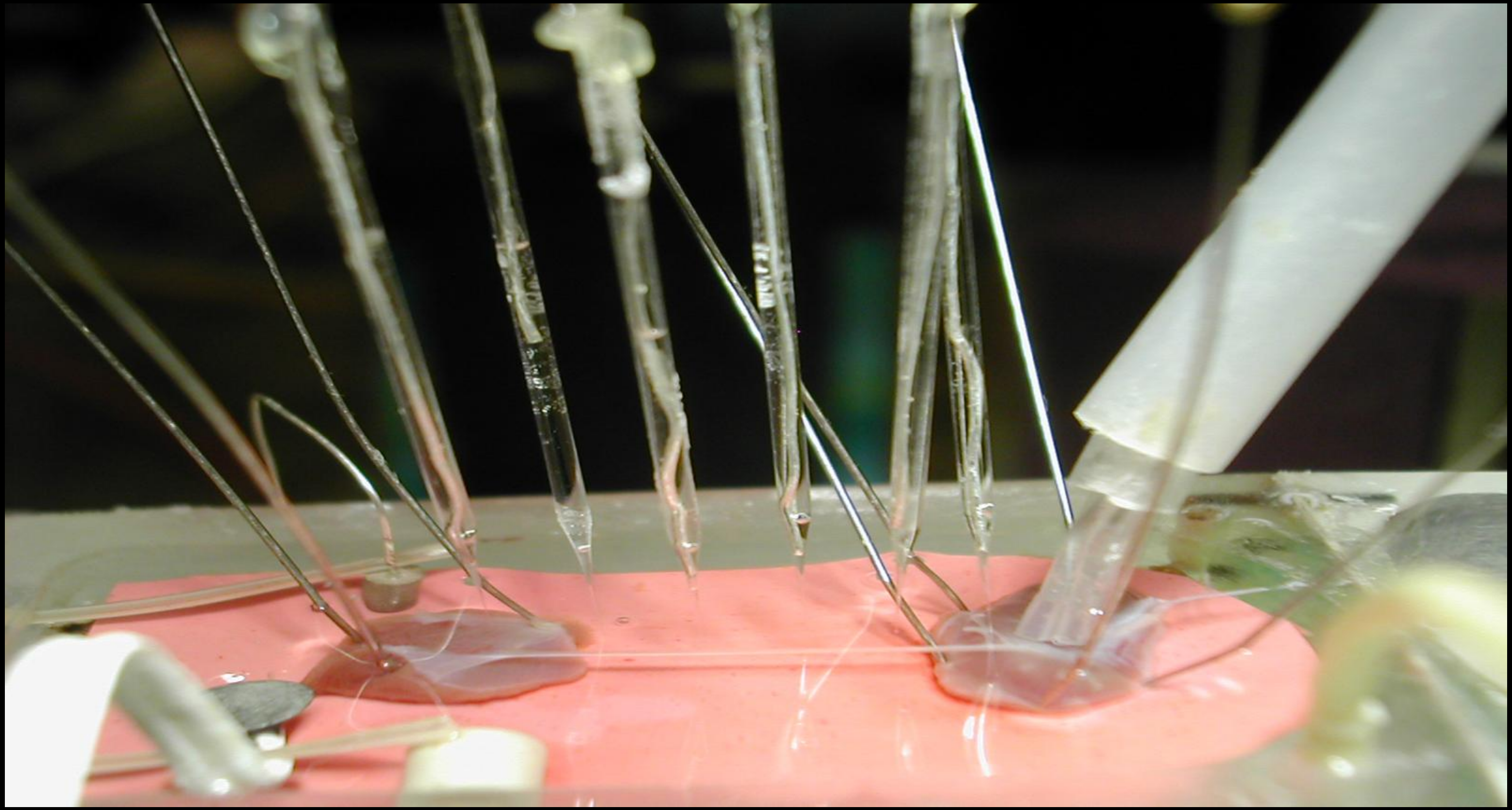

Measurements can be made using a 1D optical array
or microelectrodes.

Controlling Alternans

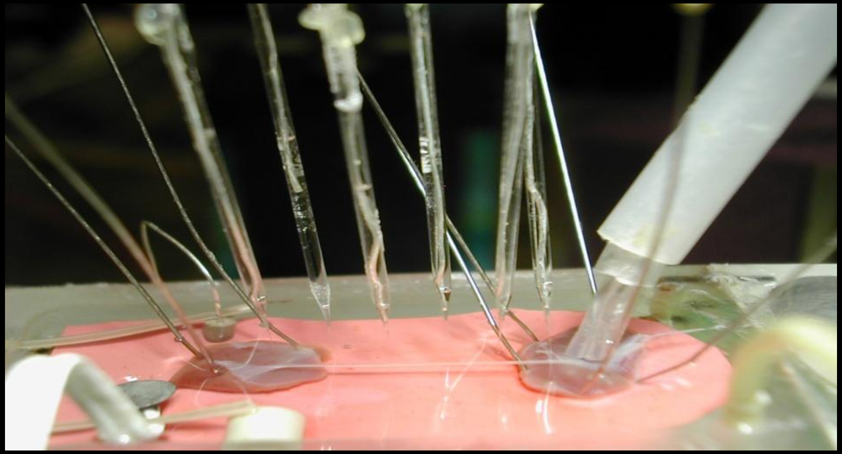

We show two of many different control schemes:

1. Varying the APD locally by current injection.
   (continuous current) $I_{ext} = \gamma\,(V(t) - V(t-\tau))\ \Theta\,(V(t) - V(t-\tau))$

$$\Theta(x) = 1 \quad \text{for } x \geq 0$$
$$= 0 \quad \text{for } x < 0$$

2. Varying the APD spatially by perturbing the stimulation period.
   (discontinuous current, applied only once every period T)

$$T_n = T^* + \Delta T \quad \text{if } \Delta T_n < 0$$
$$= T^* \quad \text{if } \Delta T_n \geq 0$$

$$\Delta T_n = \gamma\,(APD_n - APD_{n-1})$$

Rappel WJ, Fenton FH, Karma A, Phys Rev Lett 1999; 83: 456
Christini DJ et al., Phys Rev Lett 2006; 96: 104101

Controlling Alternans

$$I_{ext} = \gamma (V(t) - V(t-\tau)) \, \Theta (V(t) - V(t-\tau)$$

$$\Theta(x) = 1 \quad \text{for } x \geq 0$$
$$= 0 \quad \text{for } x < 0$$

http://thevirtualheart.org/java/controln/control.html

http://thevirtualheart.org/java/controln/control2.html

Controlling Alternans

$$T_n = T^* + \Delta T \quad \text{if } \Delta T_n < 0$$
$$\quad = T^* \quad \text{if } \Delta T_n \geq 0$$

$$\Delta T_n = \gamma\,(APD_n - APD_{n-1})$$

http://thevirtualheart.org/java/controln/controlt0.html

Using Purkinje Fibers to Study Alternans

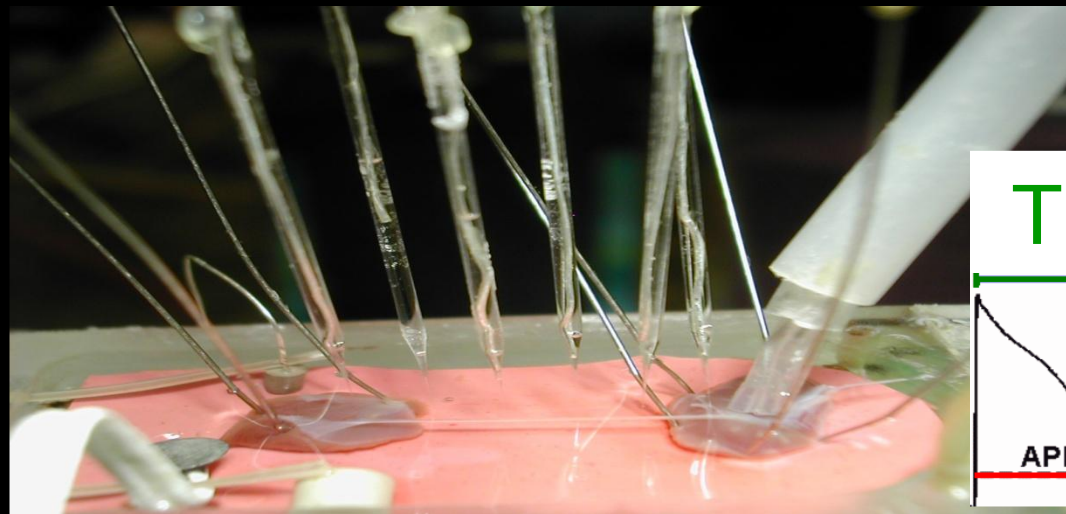

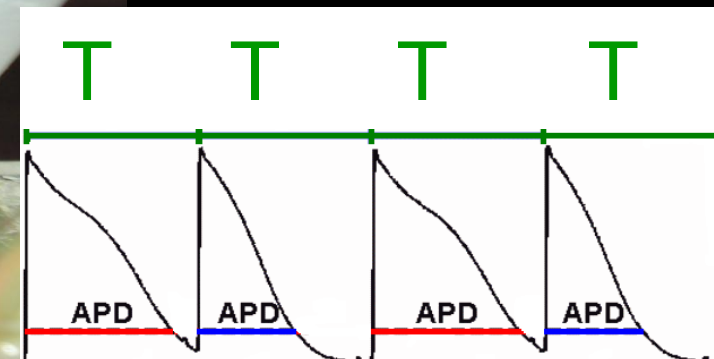

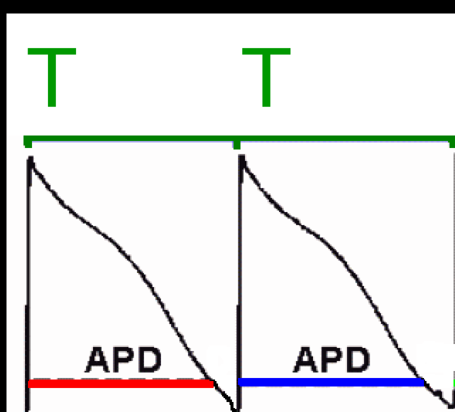

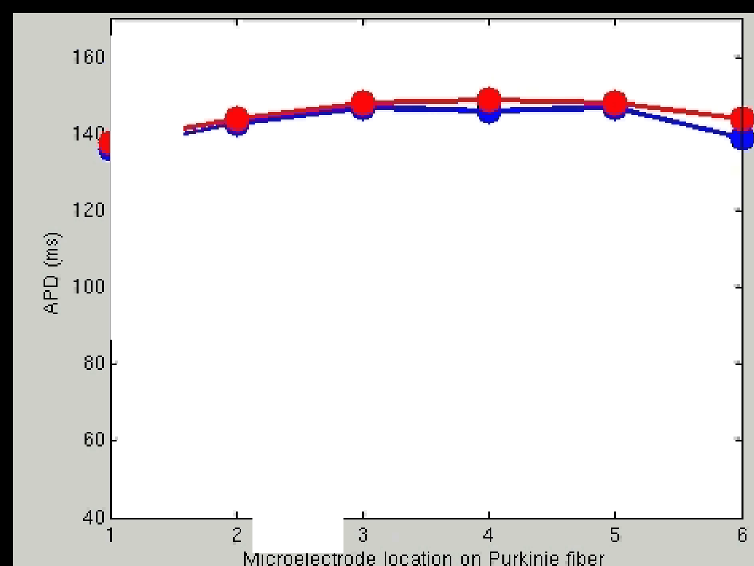

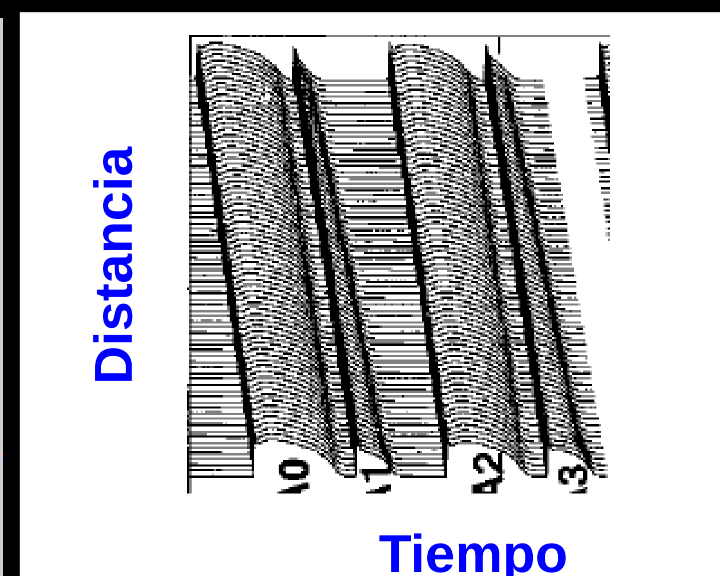

Alternacion Concordante

Using Purkinje Fibers to Study Alternans

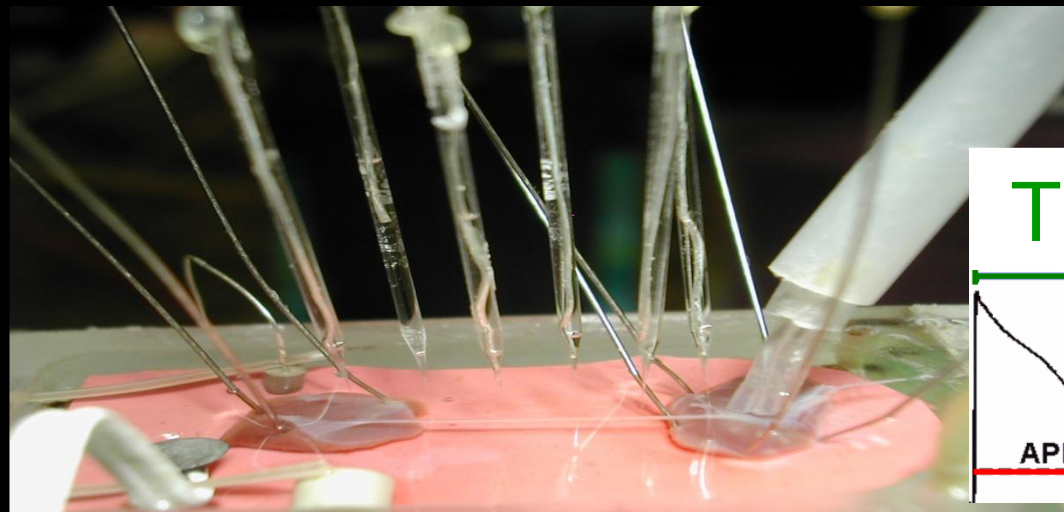

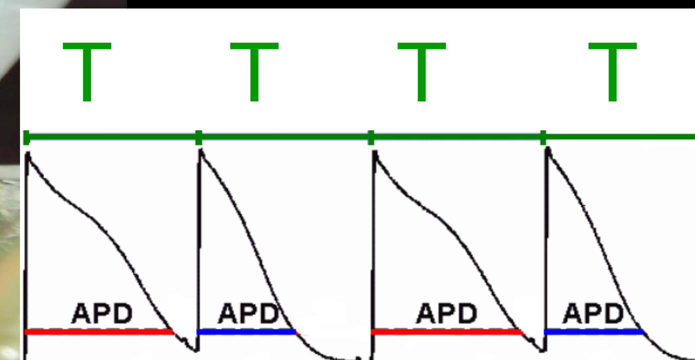

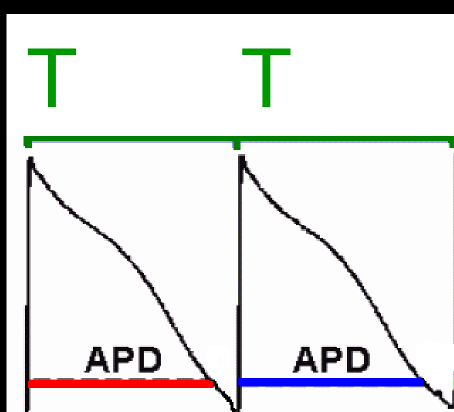

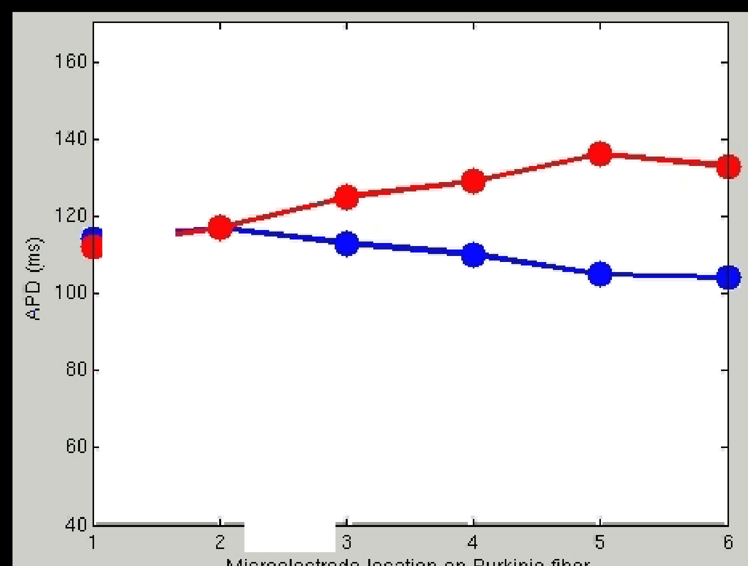

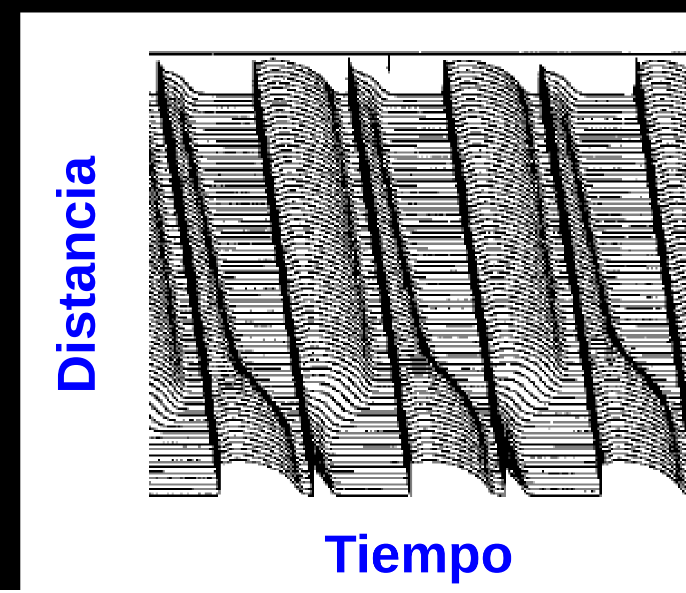

Alternacion Descordante

Control in Purkinje Fibers

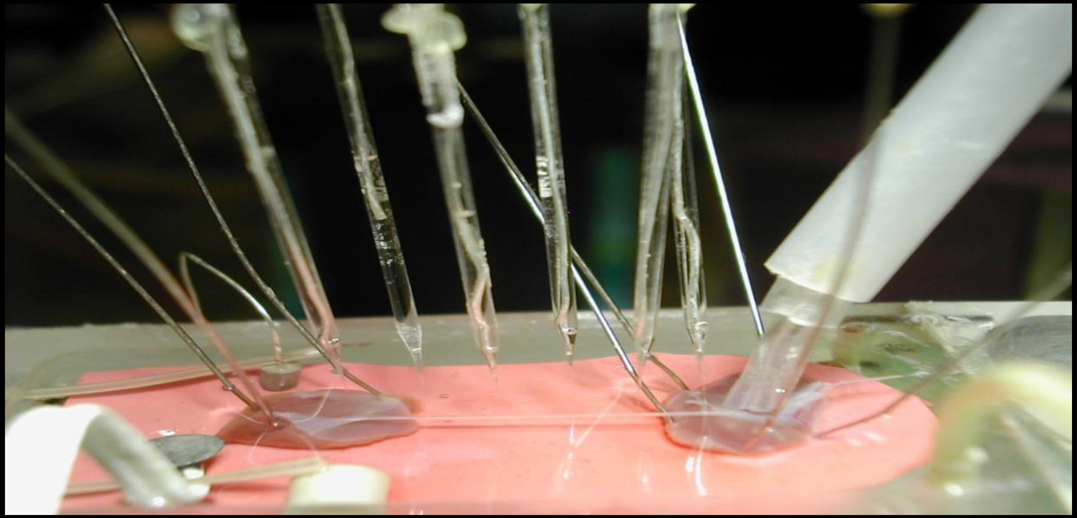

$$T_n = T^* + \Delta T \quad \text{if } \Delta T_n < 0$$
$$\quad = T^* \qquad\qquad \text{if } \Delta T_n \geq 0$$

$$\Delta T_n = \gamma\,(APD_n - APD_{n-1})$$

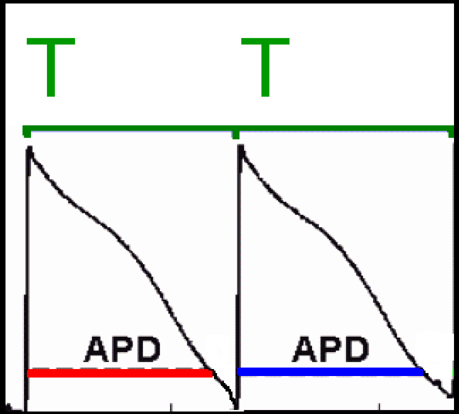

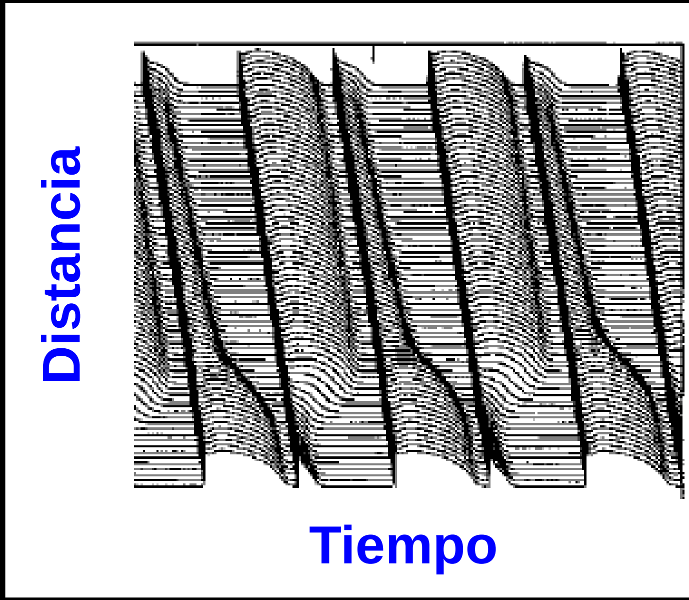

Control on spiral waves

$$I_{ext} = \gamma\,(\,V(t) - V(t\text{-}\tau)\,\theta\,(V(t) - V(t\text{-}\tau)\,)$$

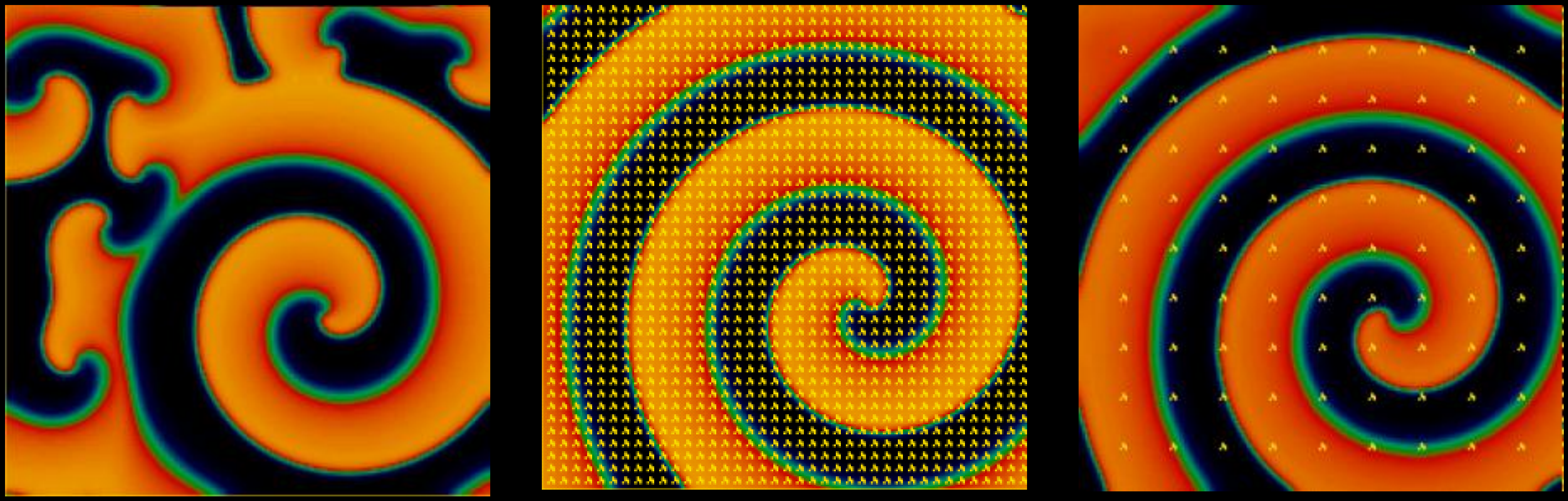

This type of control only works for control points ~ $\lambda/2$

Alternans then is very importnat.

- Problems between alternans and slope > 1 theory.

Restitution is actually a complicated property of cardiac tissue.

Some important understudied characteristics of

$\rho(DI, APD, T, CV, \xi)$

- Bifurcation (period-doubling *vs*. border collision)
- Onset of bifurcation
- Shape of AP during alternans
- Dynamic restitution
- Splitting of APD restitution
- Memory and electrotonic effects on alternans

Cherry and Fenton AJP 2004 386: H2332

Alternans in AP can be Studied in 1D strips of cardiac tissue (Purkinje fibers)

Experiments

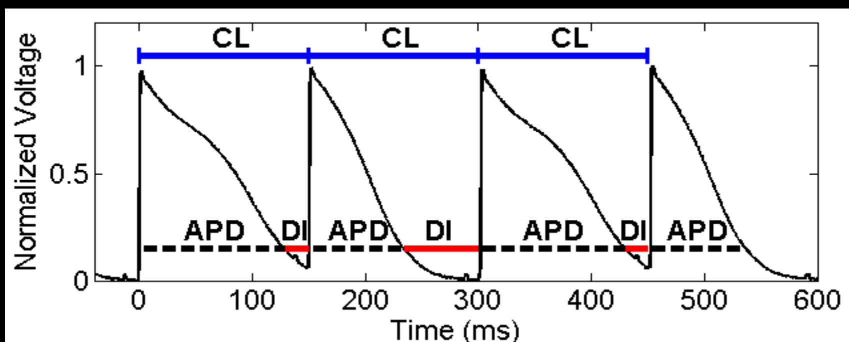

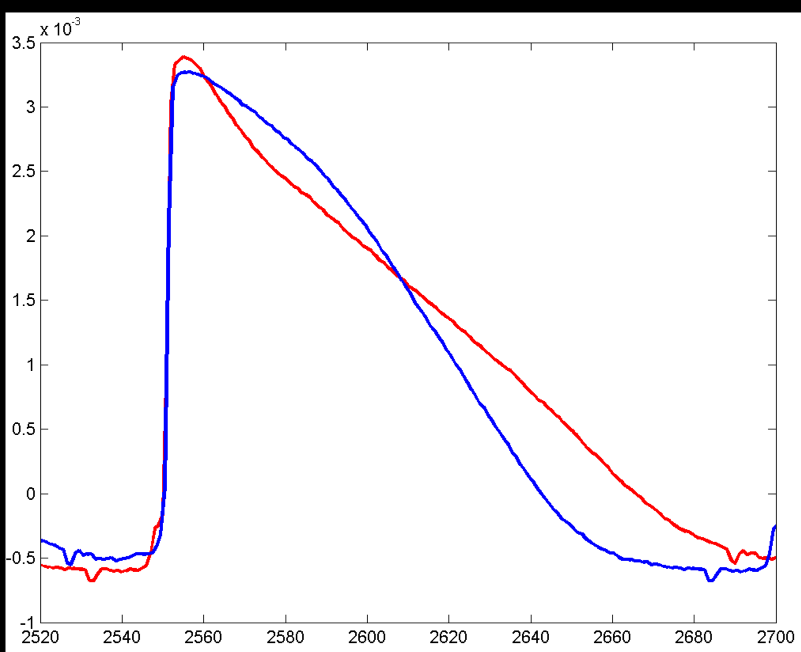

Mathematical models

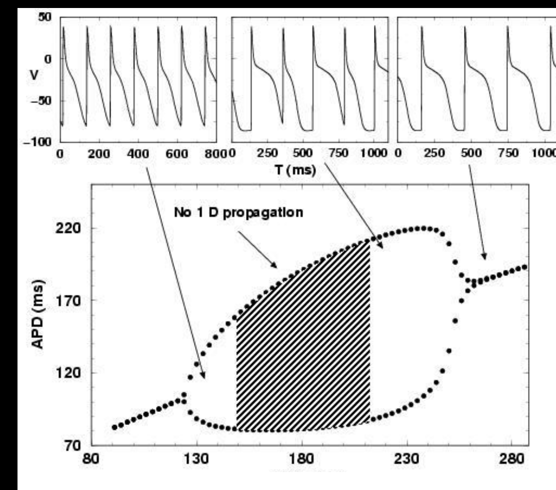

Noble model (1962)

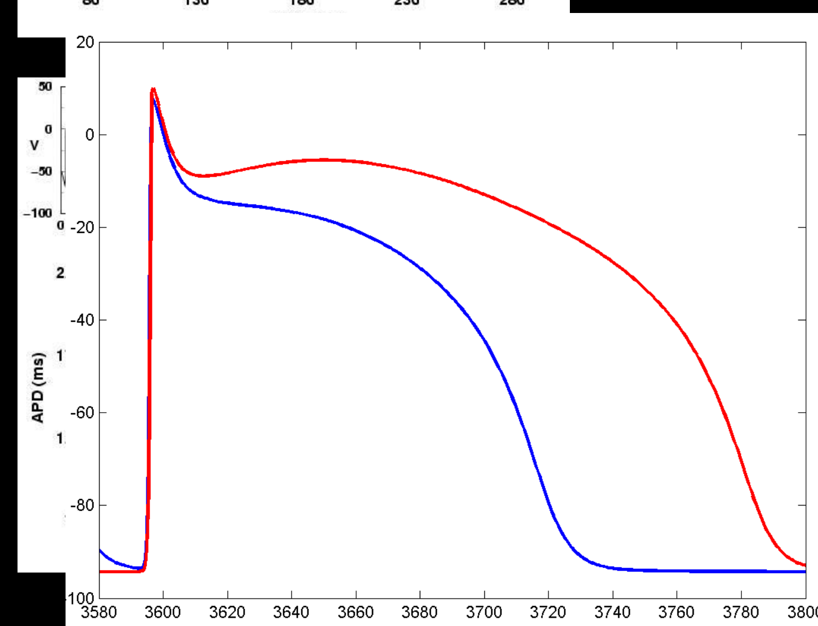

esco-
del

Period- doubling bifurcation

Pitch fork

http://thevirtualheart.org/java/Hopf2a.html

Period- doubling bifurcation
Pitch fork

http://thevirtualheart.org/java/Hopf2a.html

Border Collision bifurcation

http://thevirtualheart.org/java/Hopf2c.html

Border Collision

http://thevirtualheart.org/java/calcium/calcium.html

Possible reason for a border collision

Instability Mechanism

Steep SR-release vs. SR-load relationship induces alternans

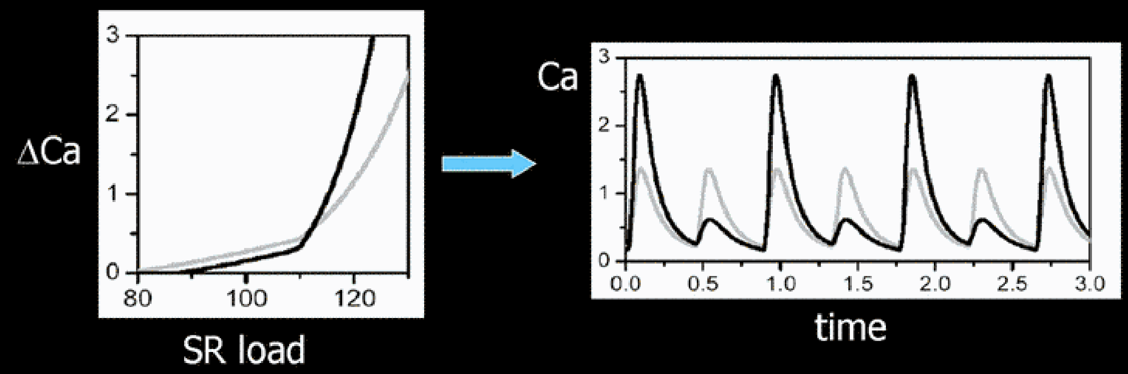

$$u = \frac{dQ(c'_j)}{dc'_j}$$ Load dependence of release

Examples of Border Collision?

Example of Border collision?

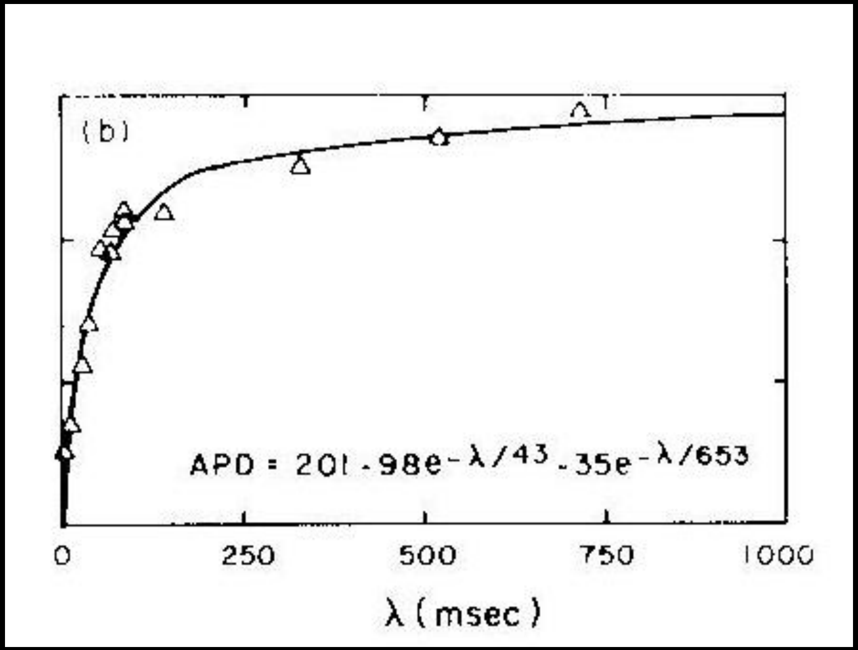

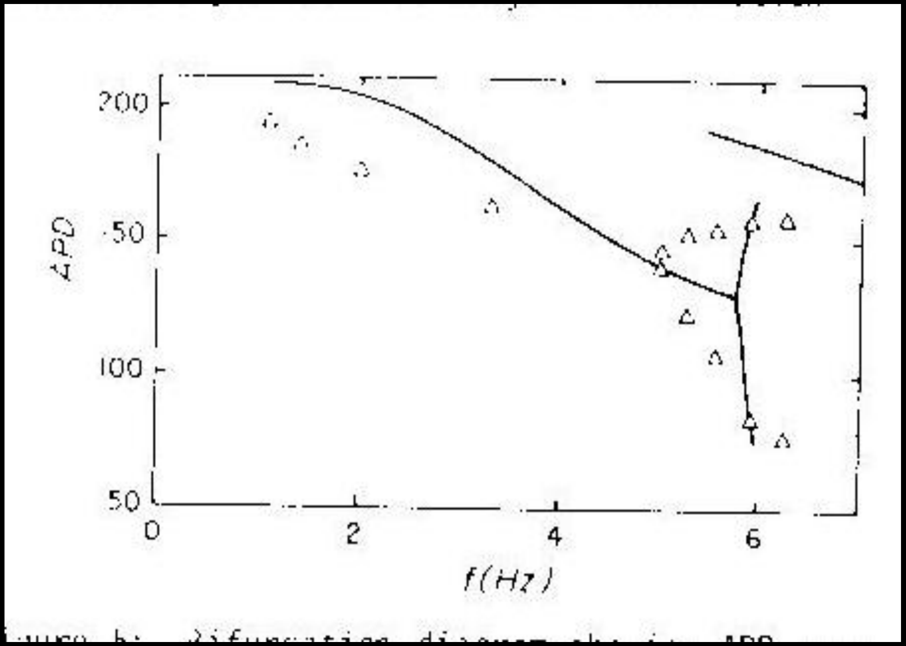

$$APD = A_0 - A_1 e^{-DI/A_2} - A_3 e^{-DI/A_4}$$

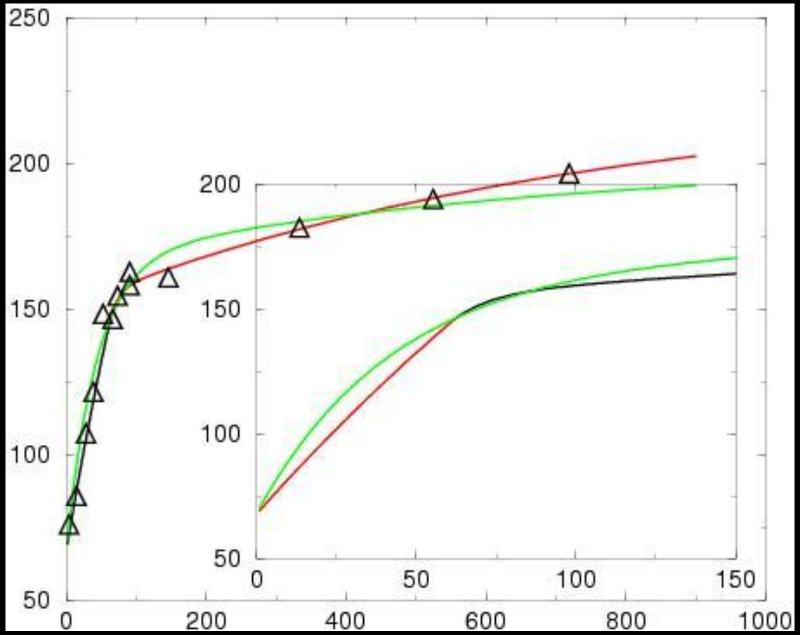

If DI > 62
A0 = 223.75
A1 = 1540.45
A2 = 12.4478
A3 =73.3533
A4 = 731.574
Else
A0 = 396.714
A1 = 329.023
A2 = 228.838
A3=A4=0

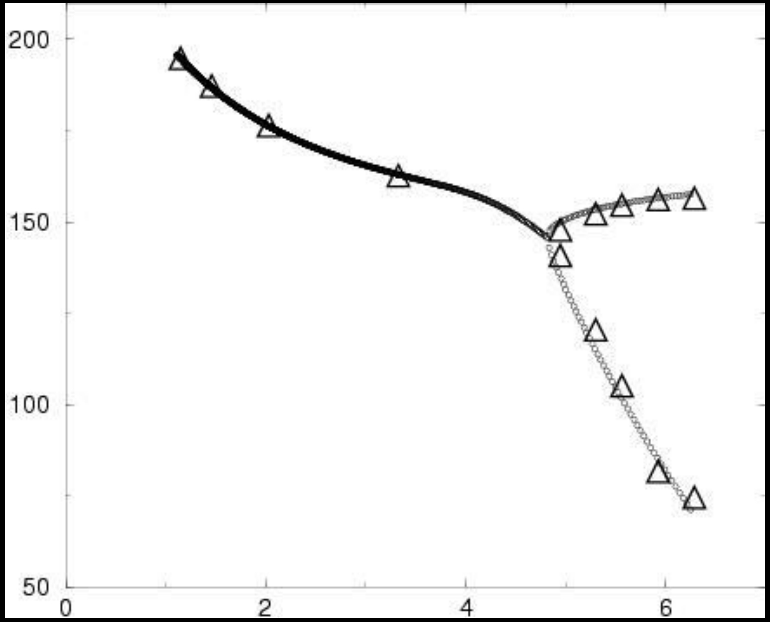

Two Important Points

1) Border collision vs. period-doubling

2) Fitting curves to data as “predictors”

$$APD = A_0 - A_1 e^{-DI/A_2} - A_3 e^{-DI/A_4}$$

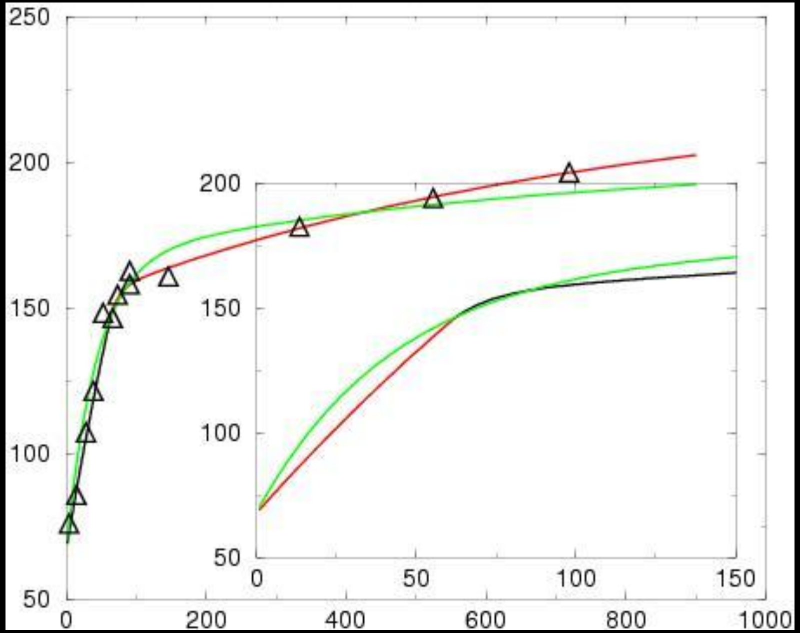

If DI > 62
A0 = 223.75
A1 = 1540.45
A2 = 12.4478
A3 =73.3533
A4 = 731.574
Else
A0 = 396.714
A1 = 329.023
A2 = 228.838
A3=A4=0

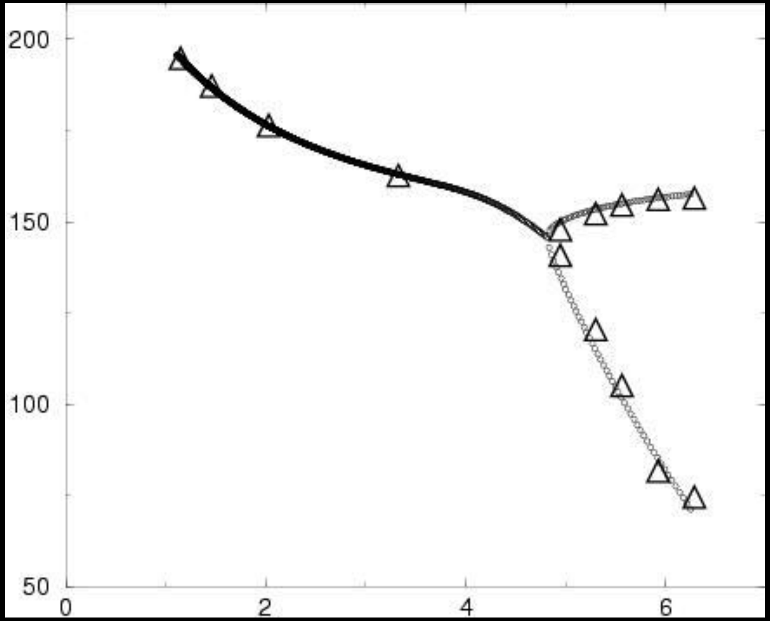

Examples of Border collision?

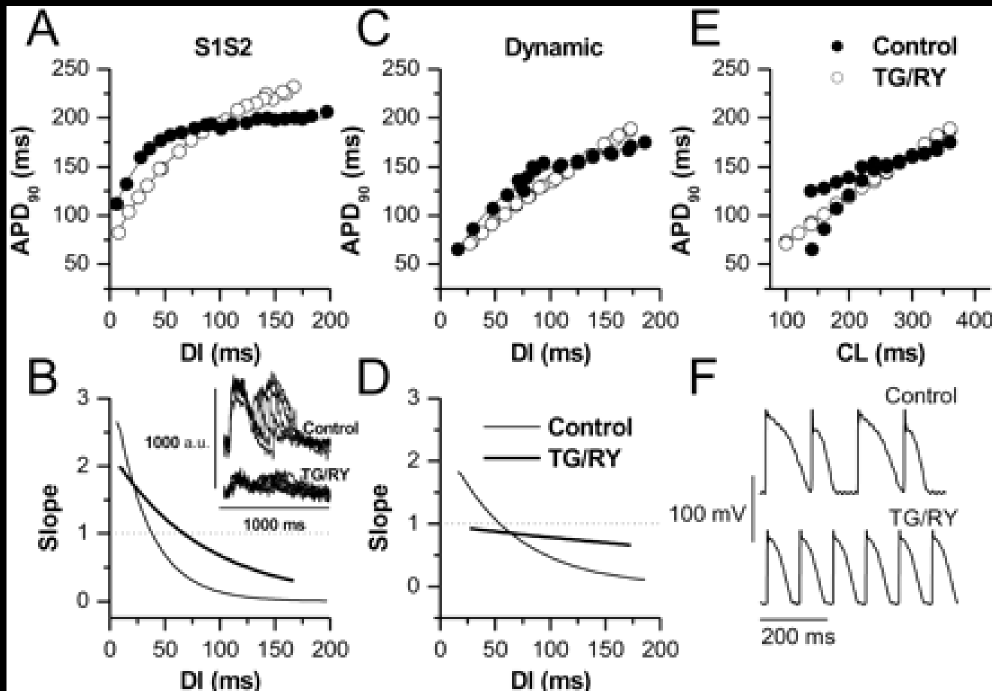

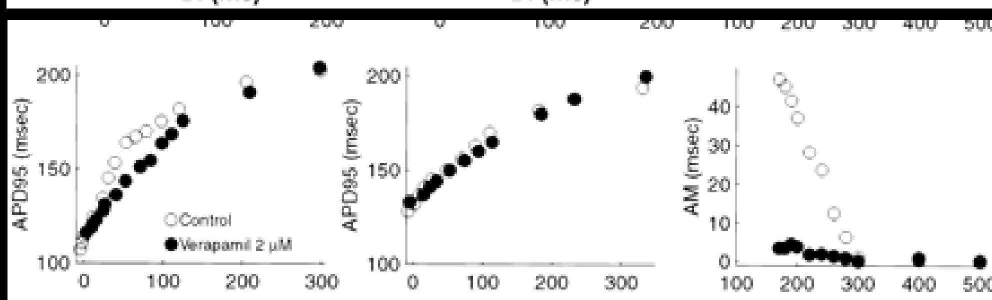

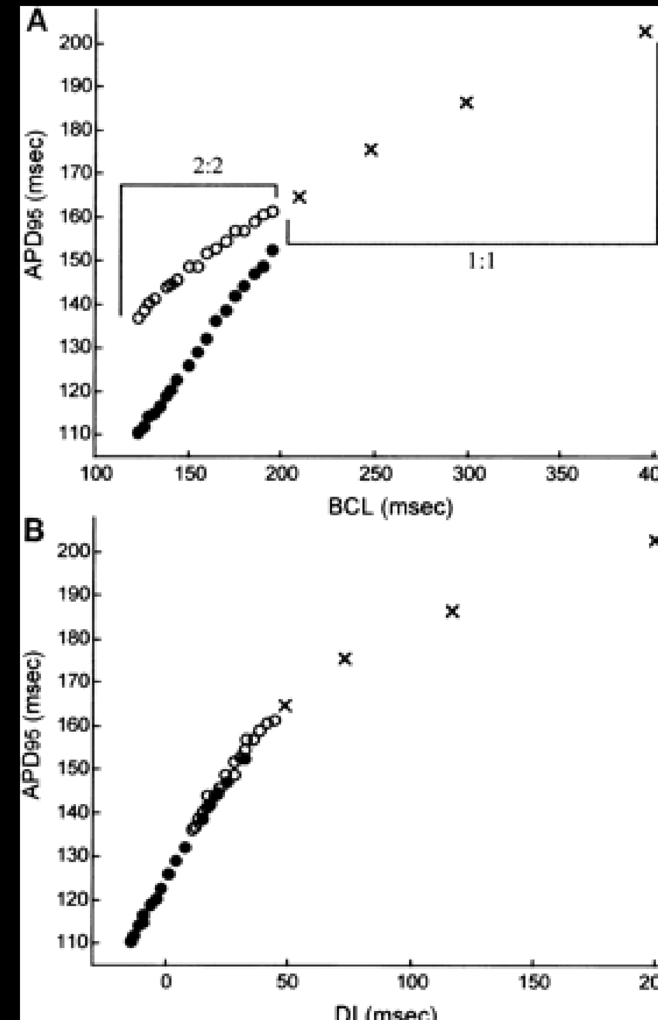

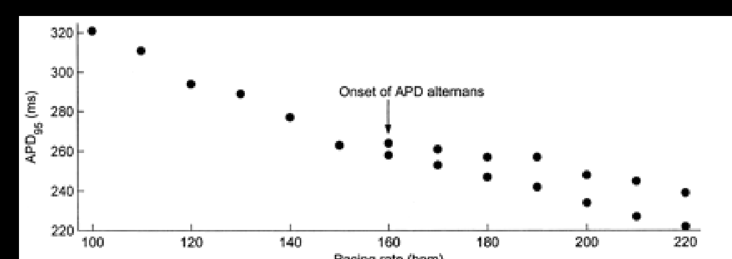

Koller et al AJP 275 H1635-H1642, 1998
Riccio et al Circ Res 955-963, 1999
Goldhaber et al. Circ Res 459-466 2005
Koller et al, Circulation 1542-1548 2005

Canine Purkinje fiber have a border collision?
Experimental and numerical study

Dog Purkinje fiber AP

APD restitution

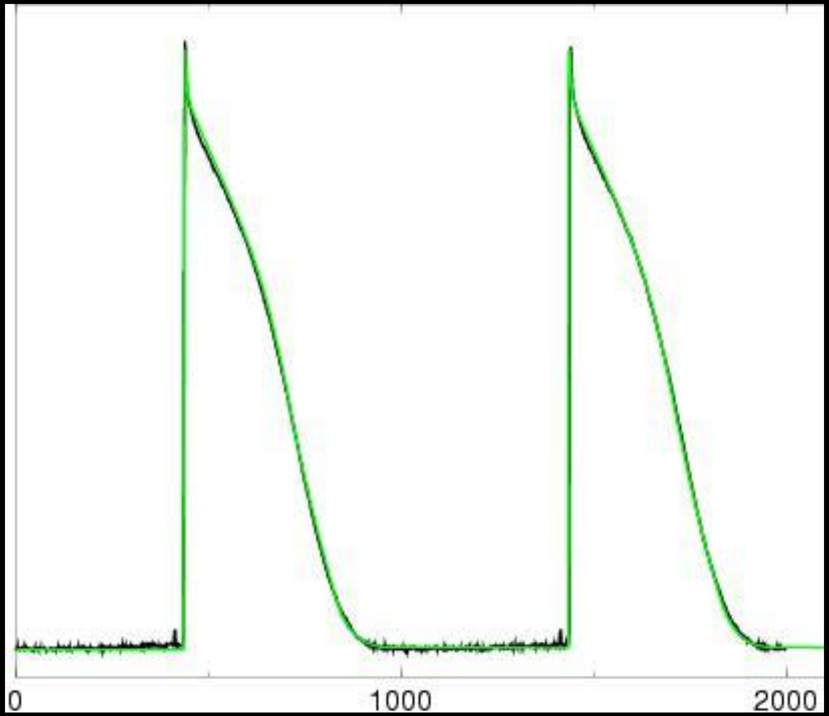

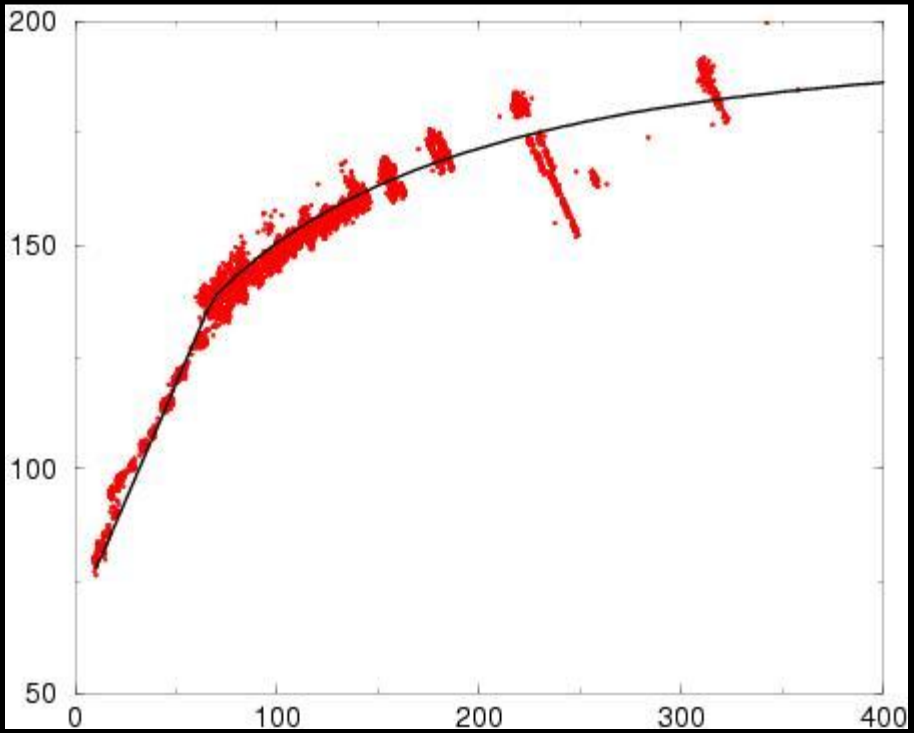

Microelectrode recording

4V model APD restitution

4V model AP

Hard to construct models
That reproduce experiments

Purkinje fiber a Border collision?

APD vs BCL

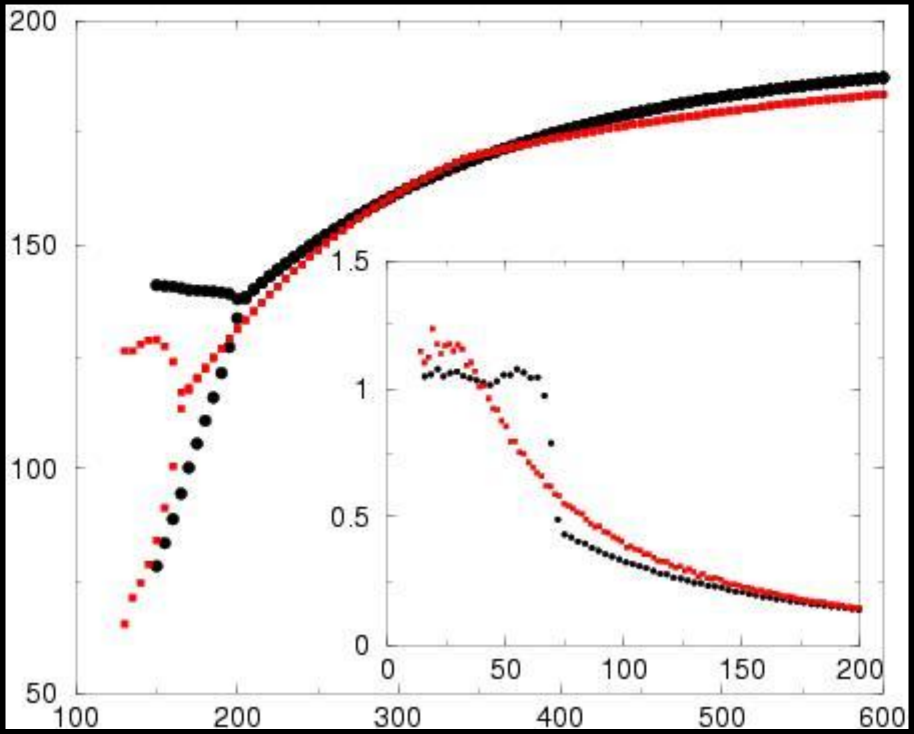

APD restitution

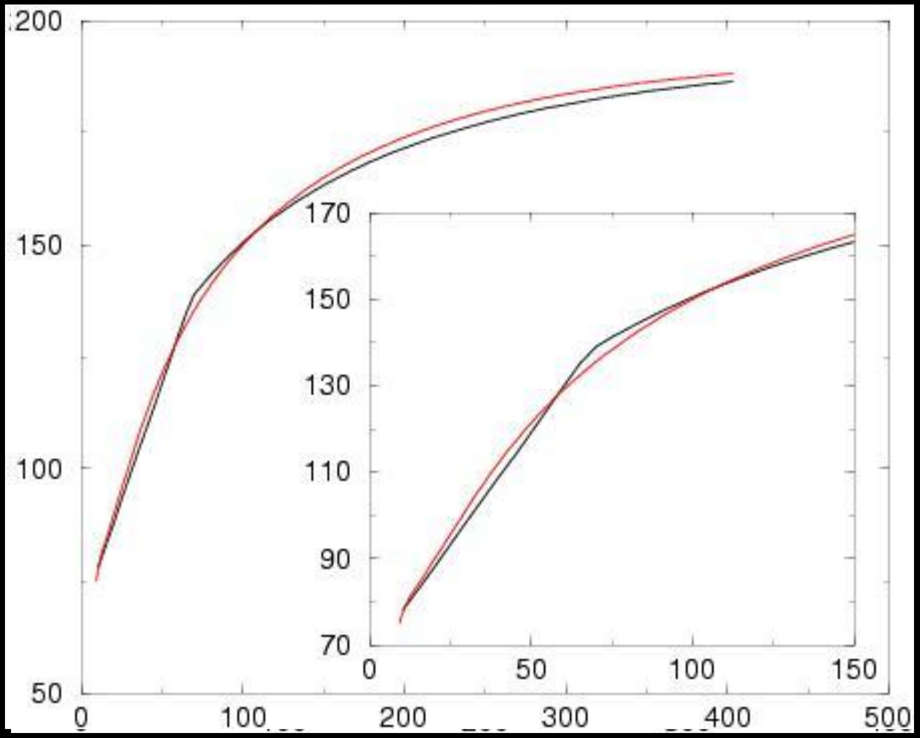

Border collision could be a possibility

Understanding the dynamics is key to produce realistic and accurate mathematical models of a system.

- We used control to prevent alternans

- How to terminate an arrhythmia?

Introduction

- Termination of Atrial arrhythmias
- Antiarrhythmic drug therapy
- Ablation
- Electrical therapies
  - ATP (effective only for slow tachycardias)
  - Electrical cardioversion (requires >5V/cm)[1]

    External ~ 100J - 280J up to 360J (1000V, 30-45 A)[3]

    Internal ~7J (350V, 4 A)[2]

1 Ideker RE, Zhou X, Knisley SB.
Pacing Clin Electrophysiol 1995;18:512-525.
2 Santini et al. J Interv Card Electrophysiol 1999;3:45-51.
3 Koster et al. Am Heart J 2004;147:e20-e26.

Introduction

- Termination of Atrial arrhythmi
- Antiarrhythmic drug therapy
- Ablation
- Electrical therapies
  - ATP (effective only for slow tachycardias)
  - Electrical cardioversion (requires >5V/cm)[1]

    External ~ 100J - 280J up to 360J (1000V, 30-45 A)[3]

    Internal ~7J (350V, 4 A)[2]

250V, 70mA, 1ms ~0.02J

1 Ideker RE, Zhou X, Knisley SB.
Pacing Clin Electrophysiol 1995;18:512-525.
2 Santini et al. J Interv Card Electrophysiol 1999;3:45-51.
3 Koster et al. Am Heart J 2004;147:e20-e26.

How Does Defibrillation Work?

Virtual Electrodes and Intrinsic Tissue Heterogeneities

Plonsey R. The nature of sources of bioelectric and biomagnetic fields. Biophys J 1982;39:309-312. → Discontinuities in conductivity can result in virtual electrodes.

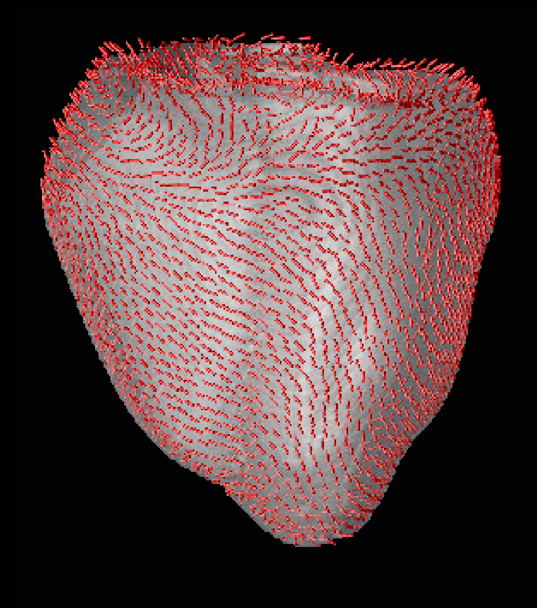

Fibers (regions where divergence is not zero)

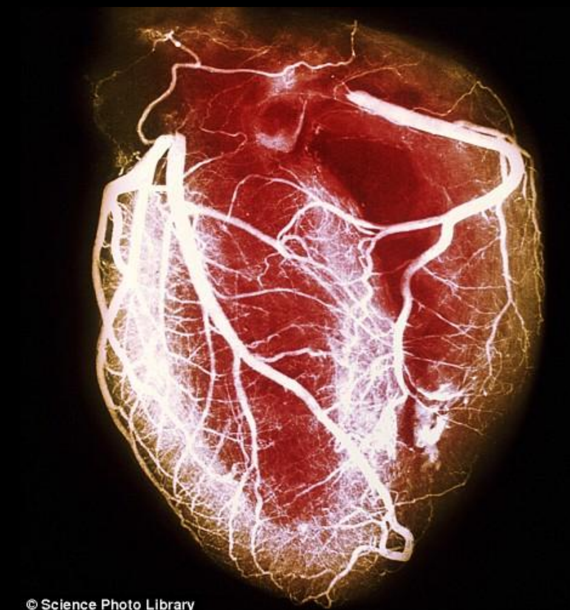

Vessels

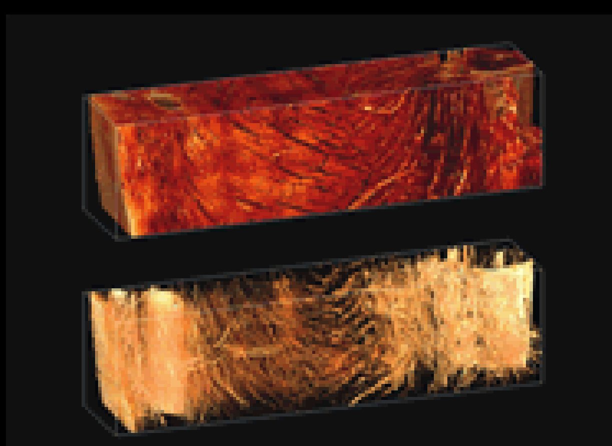

Extracellular matrix
University of Auckland

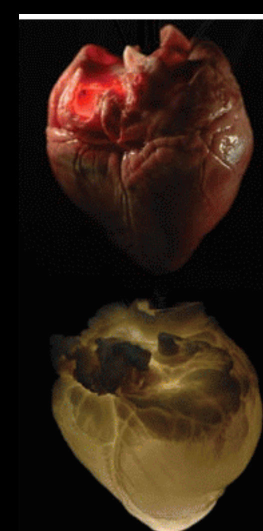

Heart stripped of all cardiac cells, extracellular matrix
University of Minnesota

Virtual Electrodes and Intrinsic Tissue Heterogeneities

Plonsey R. The nature of sources of bioelectric and biomagnetic fields. Biophys J 1982;39:309-312. → Discontinuities in conductivity can result in virtual electrodes.

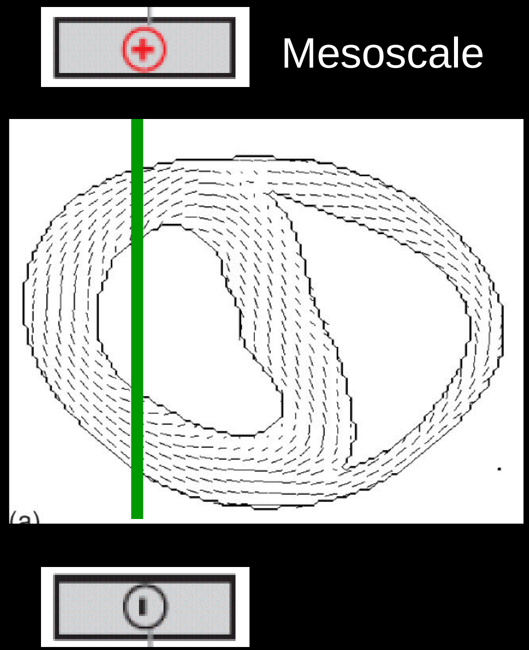

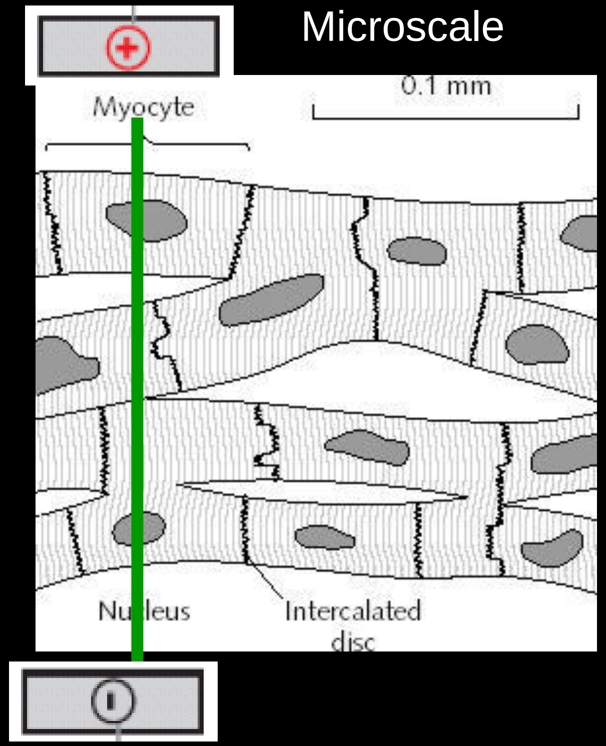

$$\nabla\cdot(D_i + D_e)\Phi_e = -\nabla\cdot(D_i \nabla V_m)$$

$$\nabla(D_i V_m) + \nabla\cdot(D_i \Delta\Phi_e) = -\beta\left(C_m \frac{\partial V_m}{\partial t} + I_{ion}\right),$$

$$V_m = \Phi_i - \Phi_e$$

When an electric field is applied current flows in the extracellular and intracellular media.

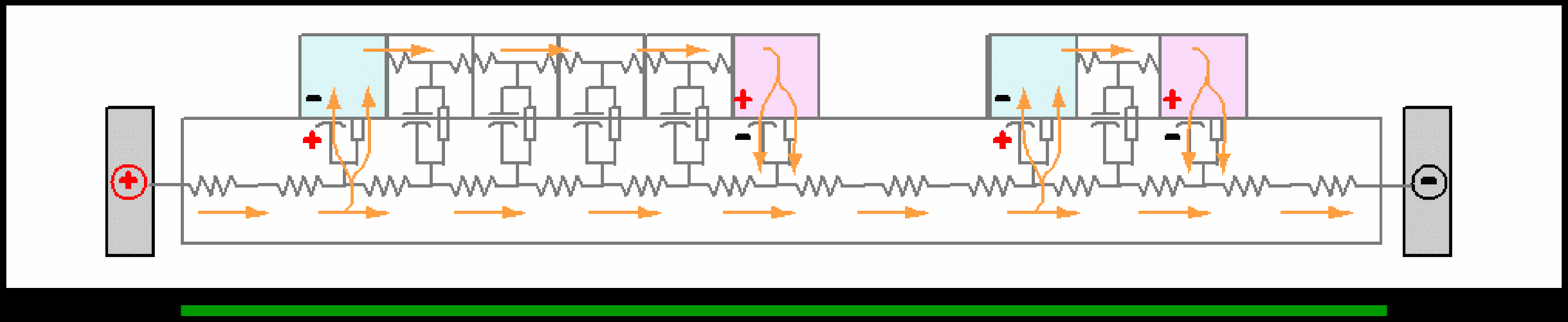

Virtual Electrodes and Intrinsic Tissue Heterogeneities

Plonsey R. The nature of sources of bioelectric and biomagnetic fields. Biophys J 1982;39:309-312. → Discontinuities in conductivity can result in virtual electrodes

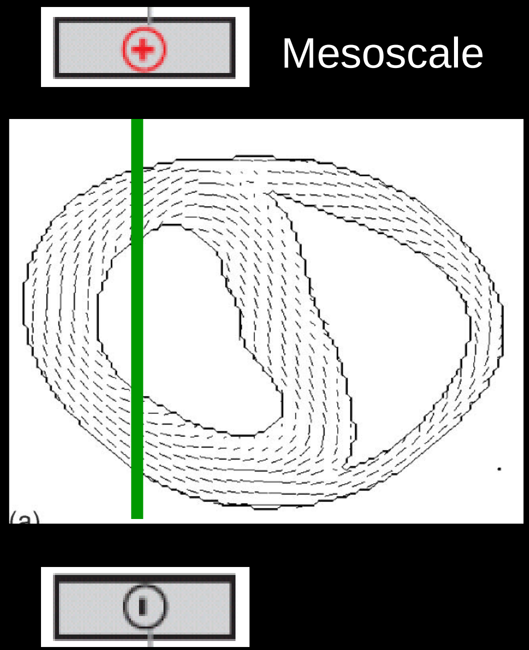

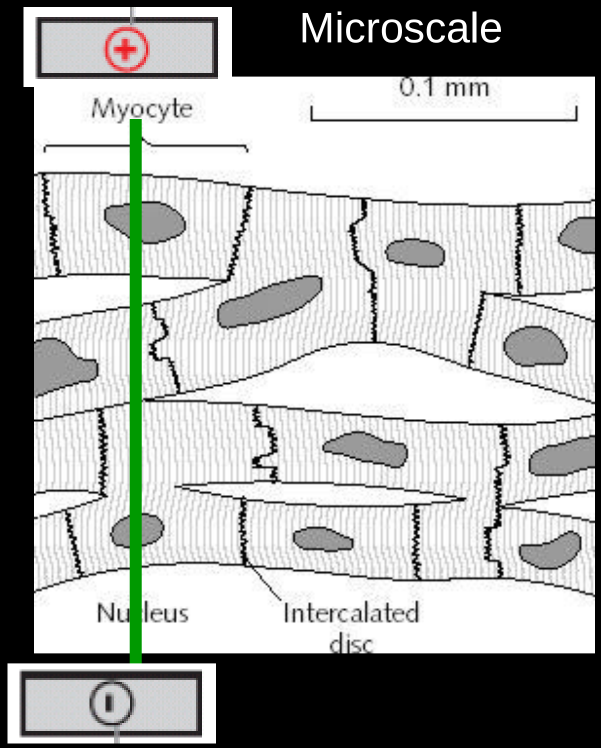

$$\nabla\cdot(D_i + D_e)\Phi_e = -\nabla\cdot(D_i\,\nabla V_m)$$

$$\nabla(D_i\,V_m) + \nabla\cdot(D_i\,\Delta\Phi_e) = -\beta\left(C_m\frac{\partial V_m}{\partial t} + I_{ion}\right),$$

$$V_m = \Phi_i - \Phi_e$$

When an electric field is applied current flows in the extracellular and intracellular media.

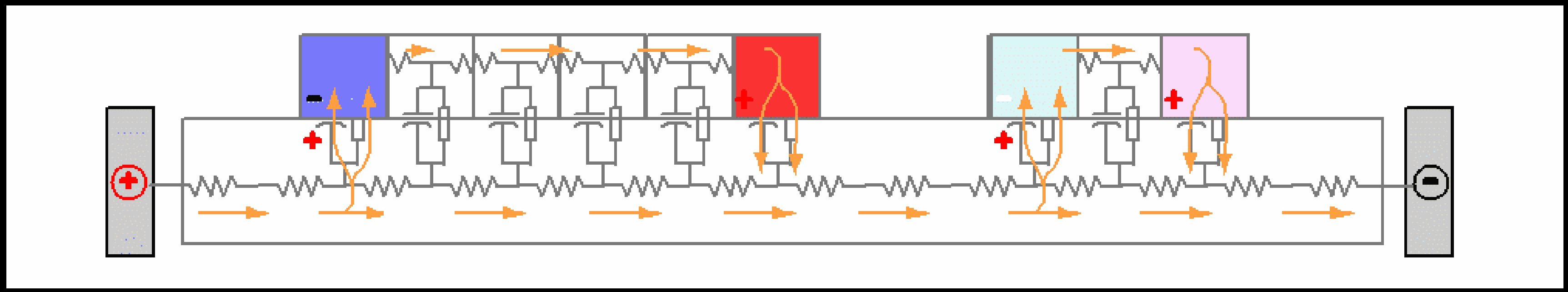

Virtual Electrodes and Intrinsic Tissue Heterogeneities

The larger the inexcitable (change in conductivity) area, the smaller the electric field strength necessary to initiate a "secondary source" or "secondary activation."

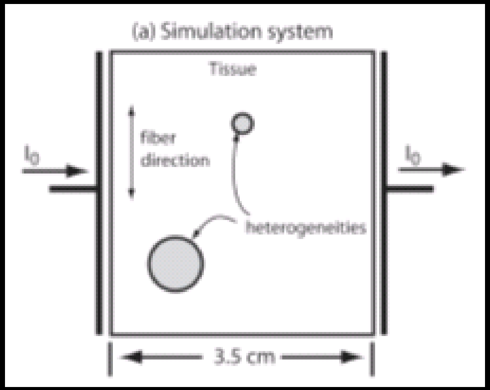

Proof of concept

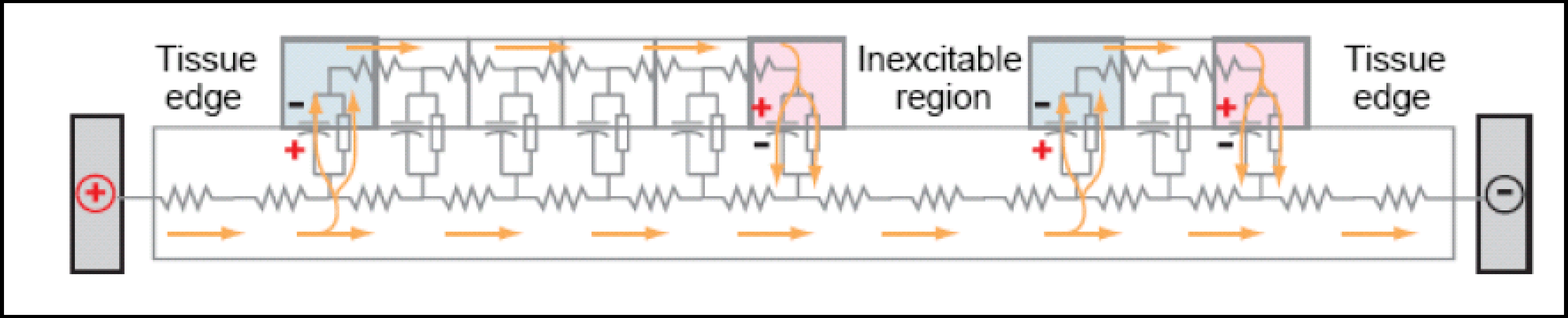

Virtual Electrodes and Intrinsic Tissue Heterogeneities

The larger the inexcitable (change in conductivity) area, the smaller the electric field strength necessary to initiate a "secondary source" or "secondary activation."

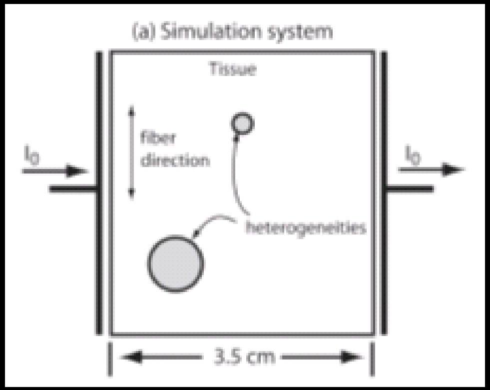

Proof of concept

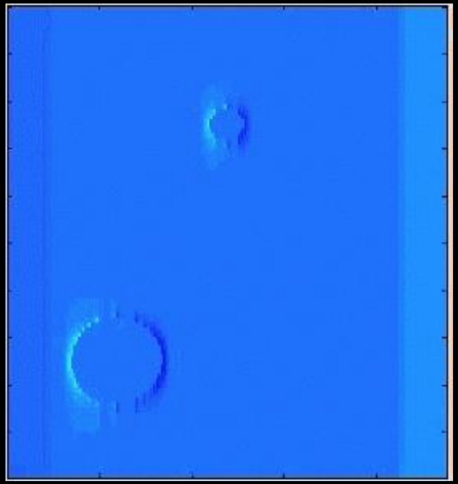

Field Strength Threshold

Bidomain (GMRES)
dx=.01 cm, dt=.01ms
Zero-flux B.C.s, phase-field
I_{ion}: Fox et al. model

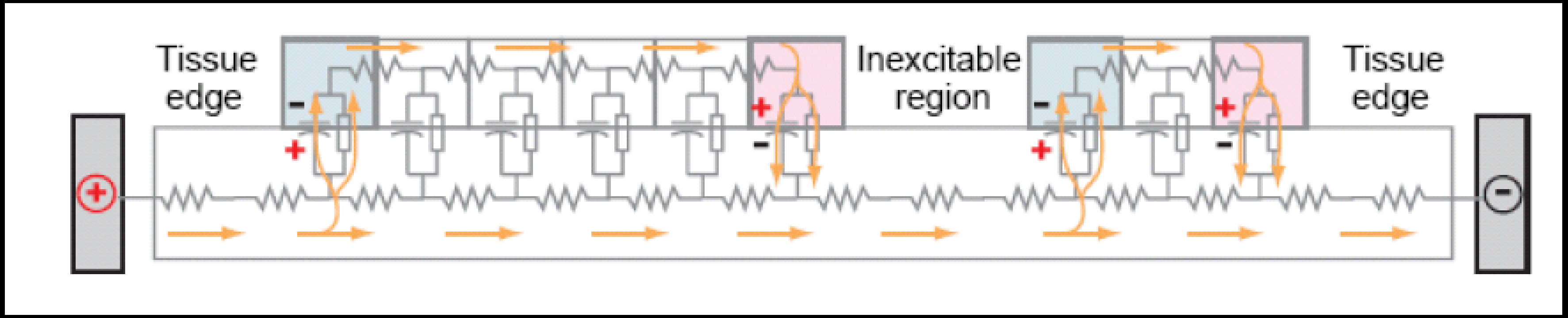

Virtual Electrodes and Intrinsic Tissue Heterogeneities

The larger the inexcitable (change in conductivity) area, the smaller the electric field strength necessary to initiate a “secondary source” or “secondary activation.”

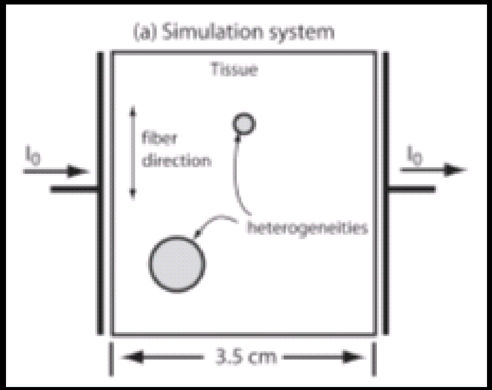

Proof of concept

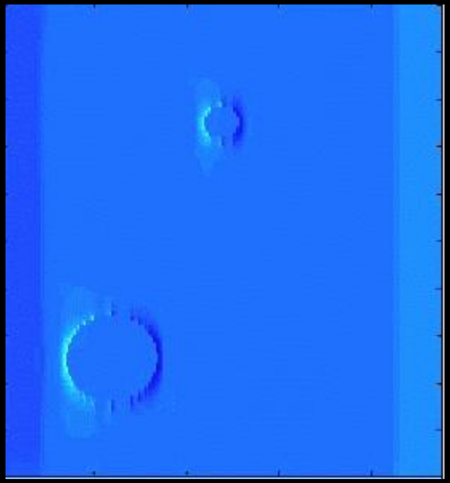

Field Strength
Low

Bidomain (GMRES)
dx=.01 cm, dt=.01ms
Zero-flux B.C.s, phase-field
I_{ion}: Fox et al. model

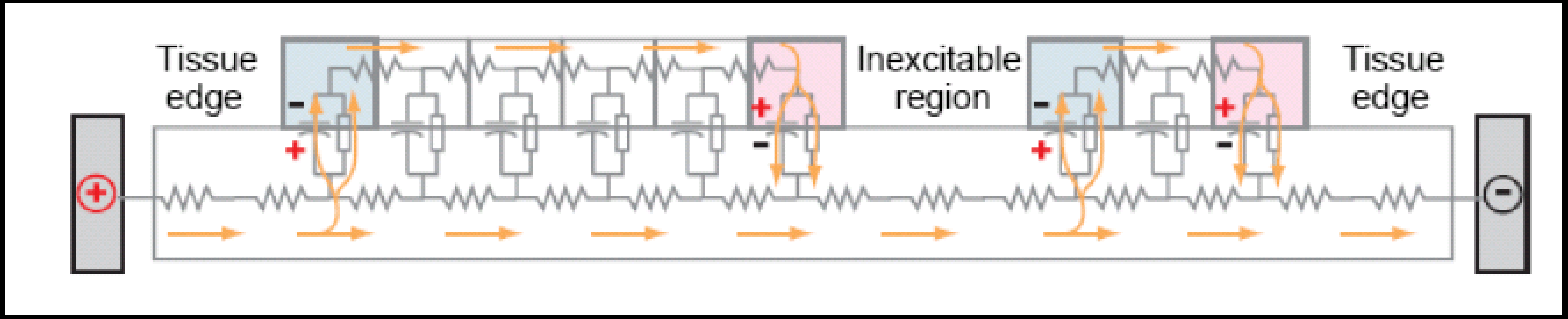

Virtual Electrodes and Intrinsic Tissue Heterogeneities

The larger the inexcitable (change in conductivity) area, the smaller the electric field strength necessary to initiate a "secondary source" or "secondary activation." (more than size, ~solid angle)

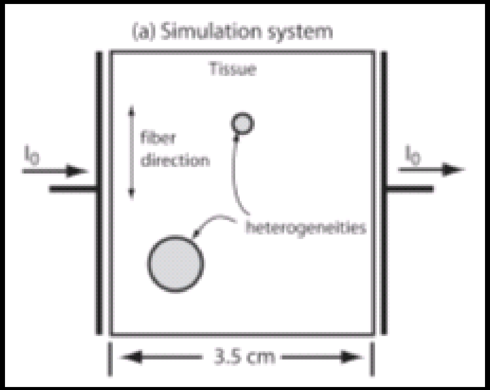

Proof of concept

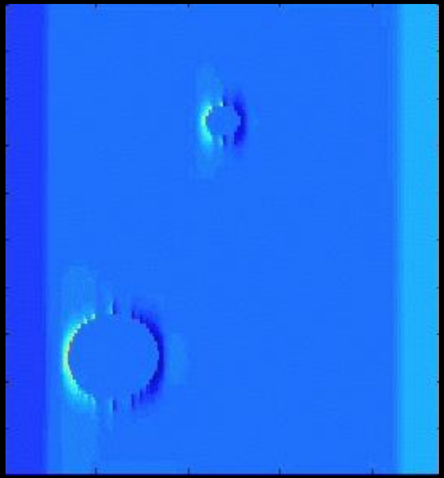

Field Strength
Medium

Bidomain (GMRES)
dx=.01 cm, dt=.01ms
Zero-flux B.C.s, phase-field
I_{ion}: Fox et al. model

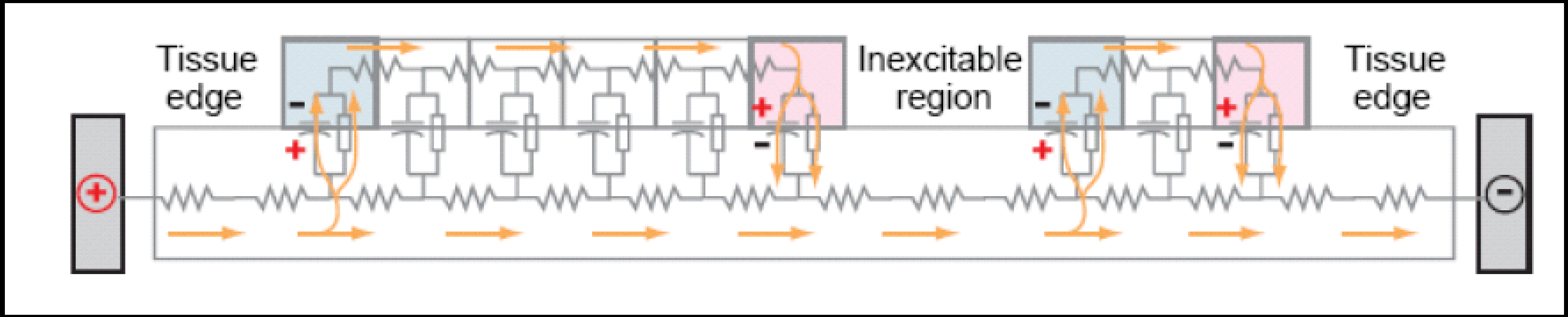

Virtual Electrodes and Intrinsic Tissue Heterogeneities

The larger the inexcitable (change in conductivity) area, the smaller the electric field strength necessary to initiate a "secondary source."

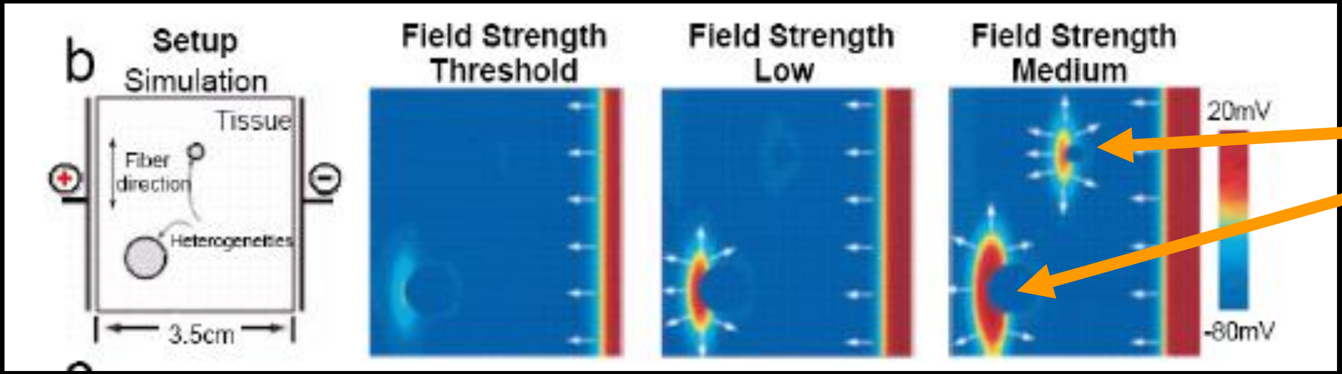

"Virtual electrodes"
and
Secondary sources

Virtual Electrodes and Intrinsic Tissue Heterogeneities

The larger the inexcitable (change in conductivity) area, the smaller the electric field strength necessary to initiate a "secondary source."

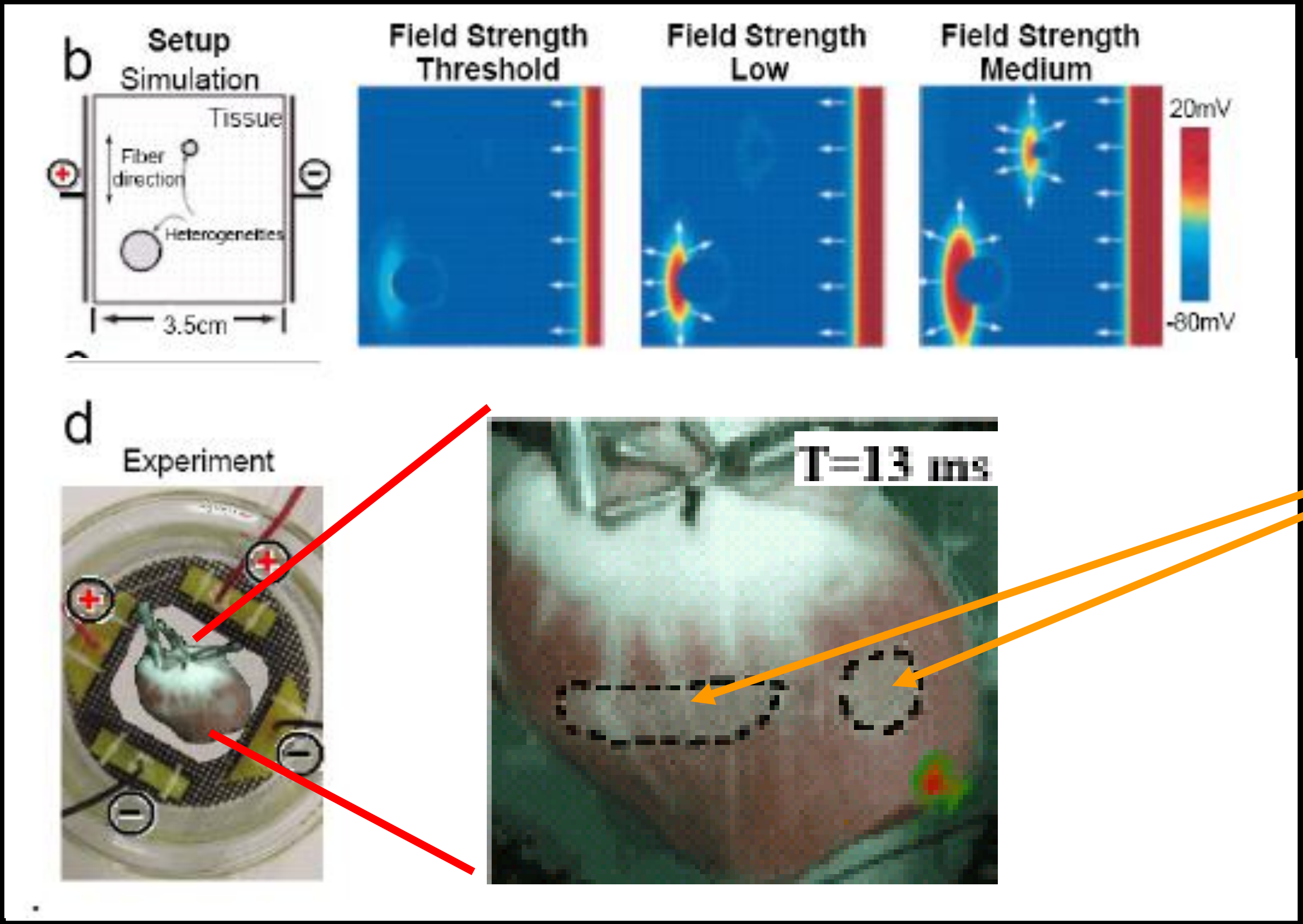

Proof of concept (experimental)
Cryoablation and optical mapping

Virtual Electrodes and Secondary Sources

The larger the inexcitable (change in conductivity) area, the smaller the electric field strength necessary to initiate a “secondary source.”

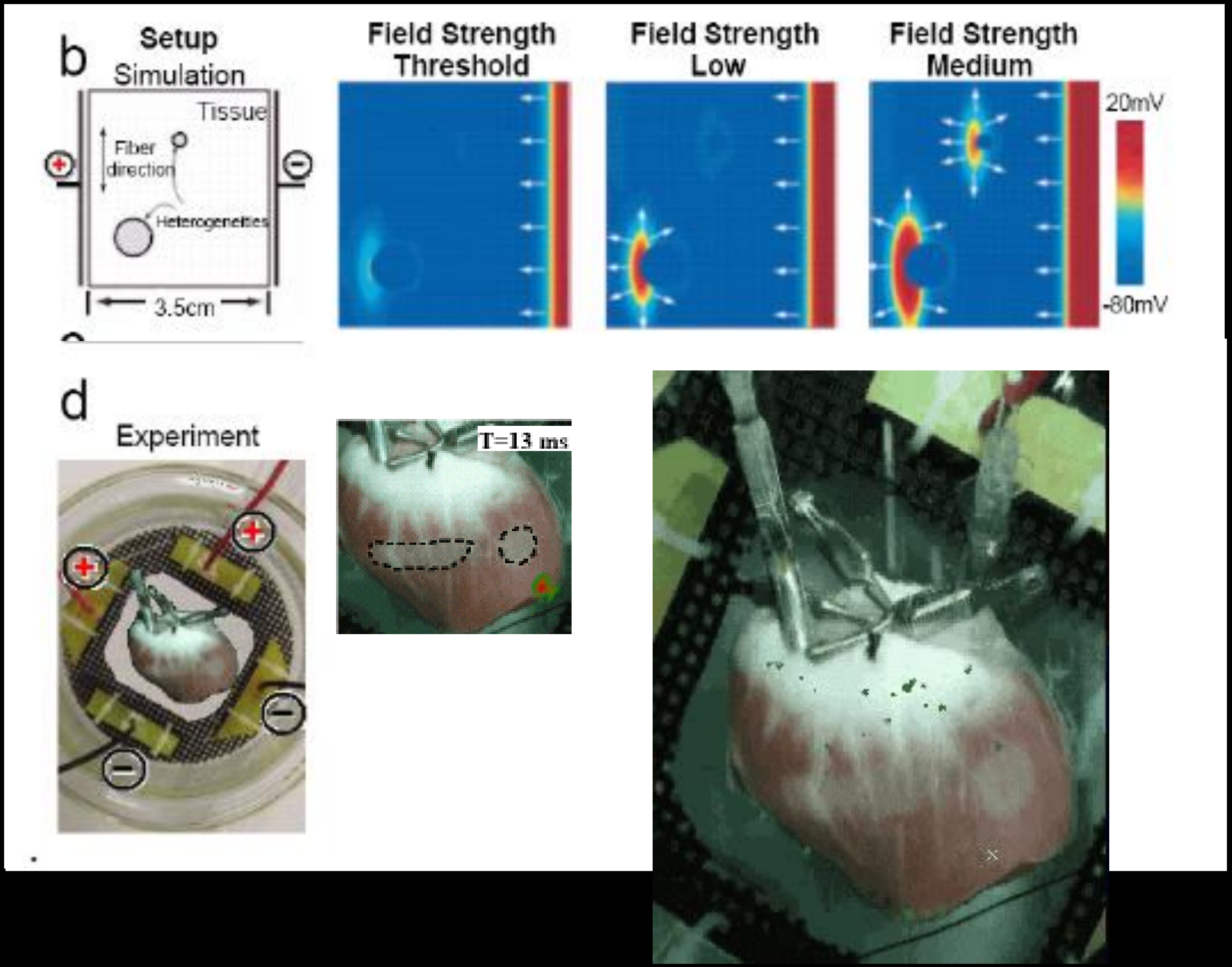

Field Strength
$E = 0.18$ V/cm

Virtual Electrodes and Secondary Sources

The larger the inexcitable (change in conductivity) area, the smaller the electric field strength necessary to initiate a "secondary source."

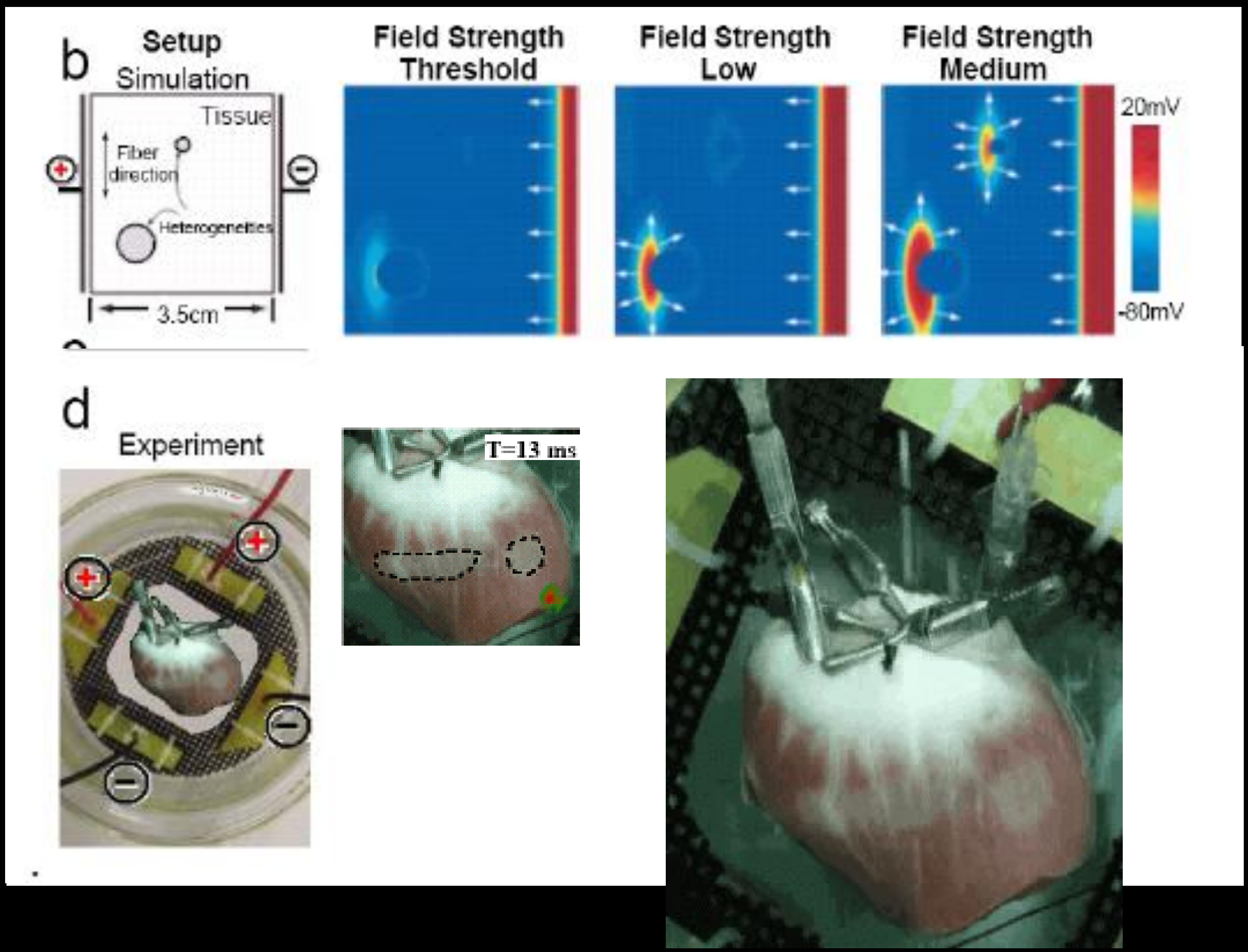

Field Strength
E = 0.56 V/cm

Virtual Electrodes and Secondary Sources

The larger the inexcitable (change in conductivity) area, the smaller the electric field strength necessary to initiate a “secondary source.”

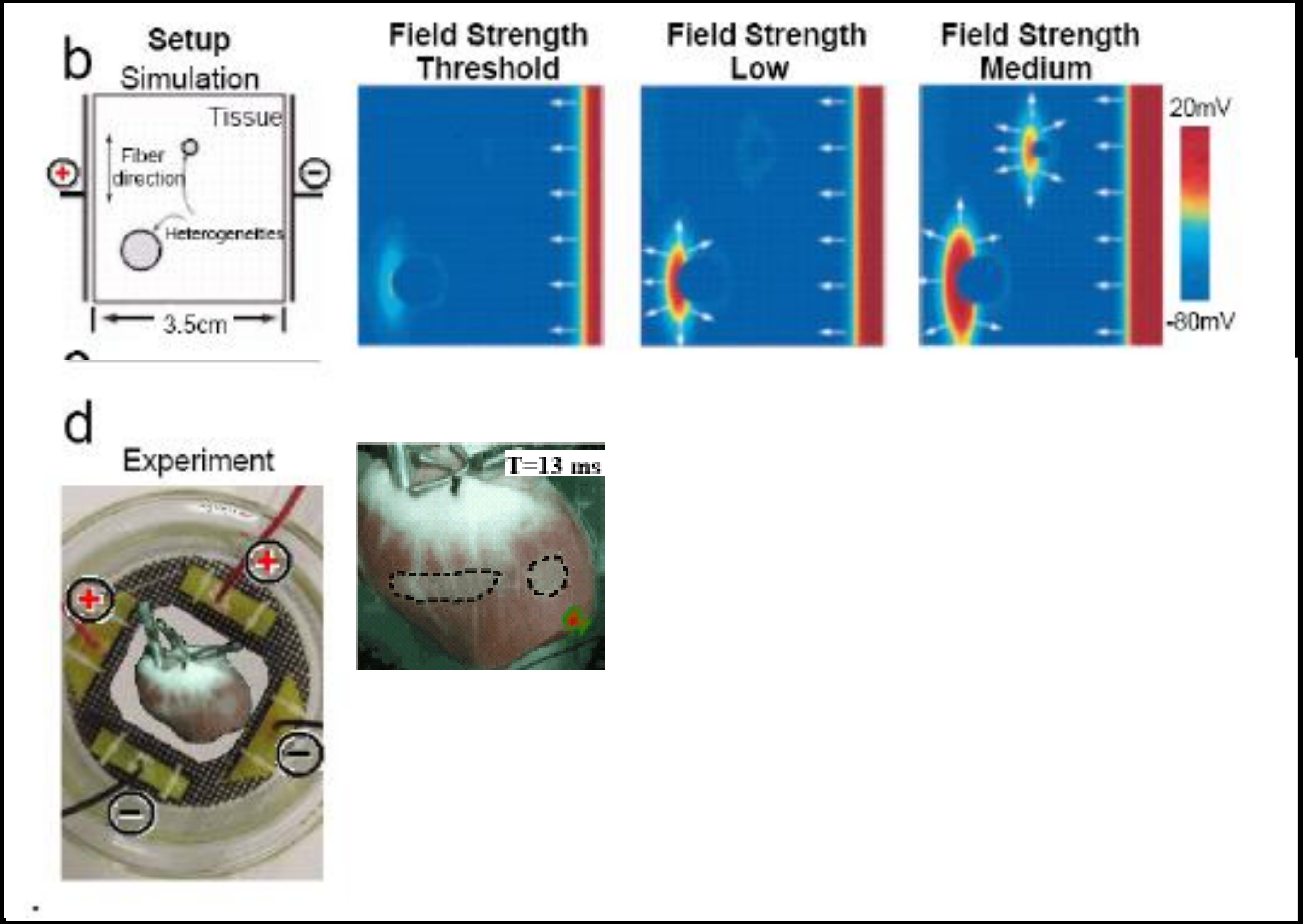

Virtual Electrodes and Secondary Sources

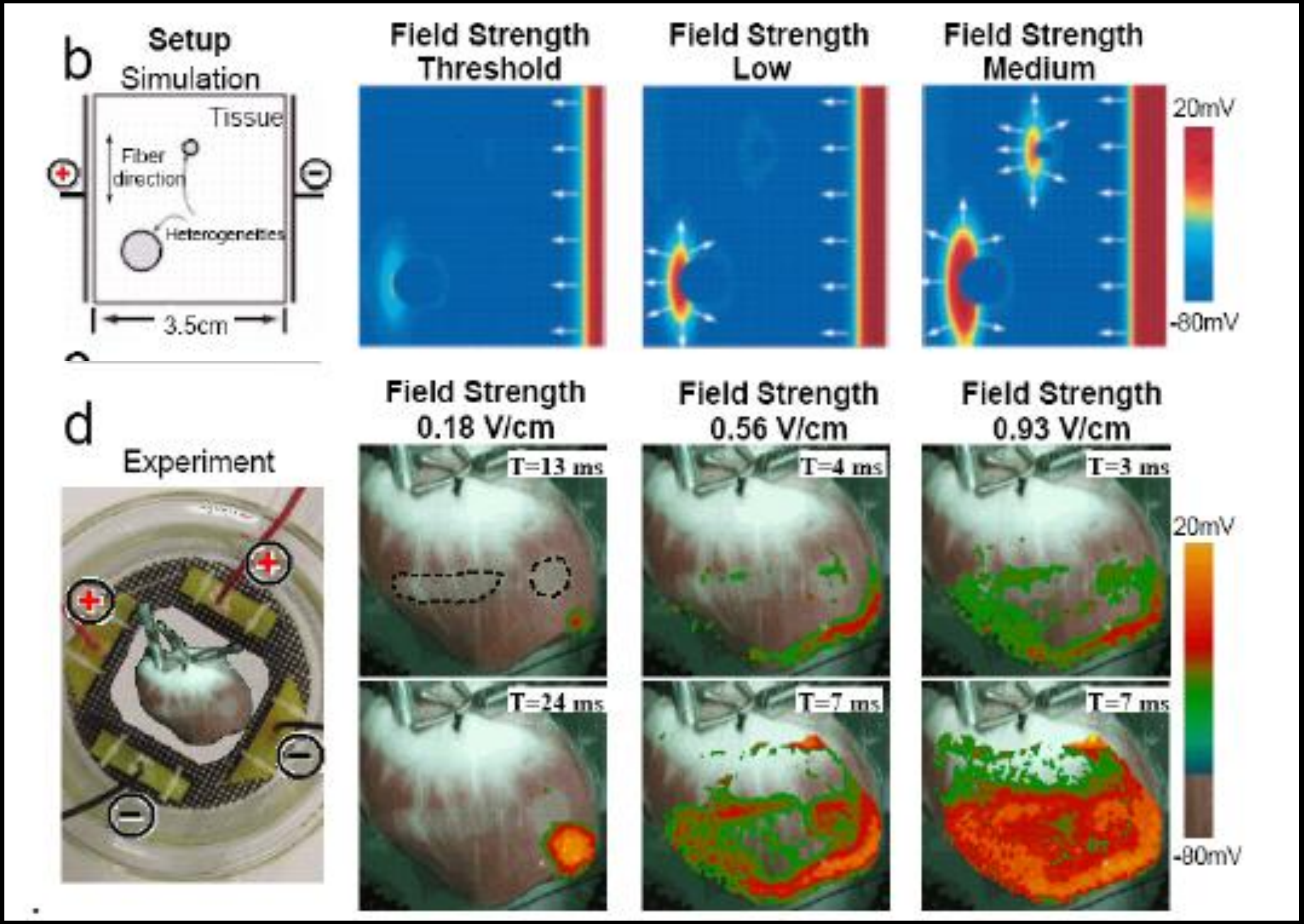

Virtual Electrodes and Secondary Sources

Example with large holes was a proof of concept.

Not only large holes but also smaller conductivity discontinuities can act as "virtual electrodes."

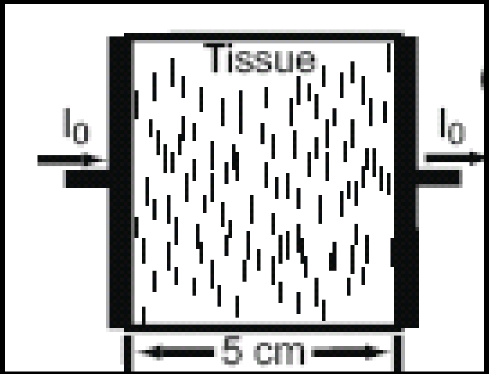

Virtual Electrodes and Secondary Sources

Example with large holes was a proof of concept

Not only large holes but also smaller conductivity discontinuities can act as "virtual electrodes."

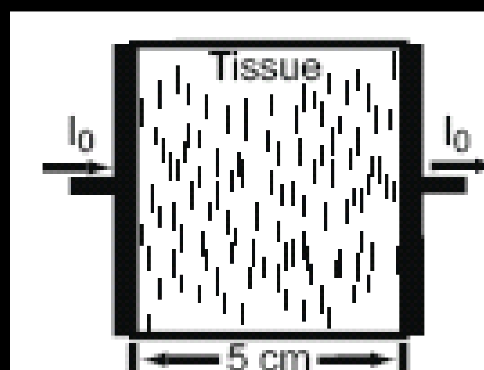

Field Strength
E = 0.6 V/cm

Field Strength
E = 1.2 V/cm

Bidomain (GMRES)
dx=.01 cm, dt=.01ms
Zero-flux B.C.s, finite-volume
I_{ion}: Fox et al. model
Collagen ~.065cm

Virtual Electrodes and Secondary Sources

Any conductivity discontinuities can act as "virtual electrodes" and activate the tissue.

The more "virtual electrodes" recruited, the faster the whole tissue is excited.

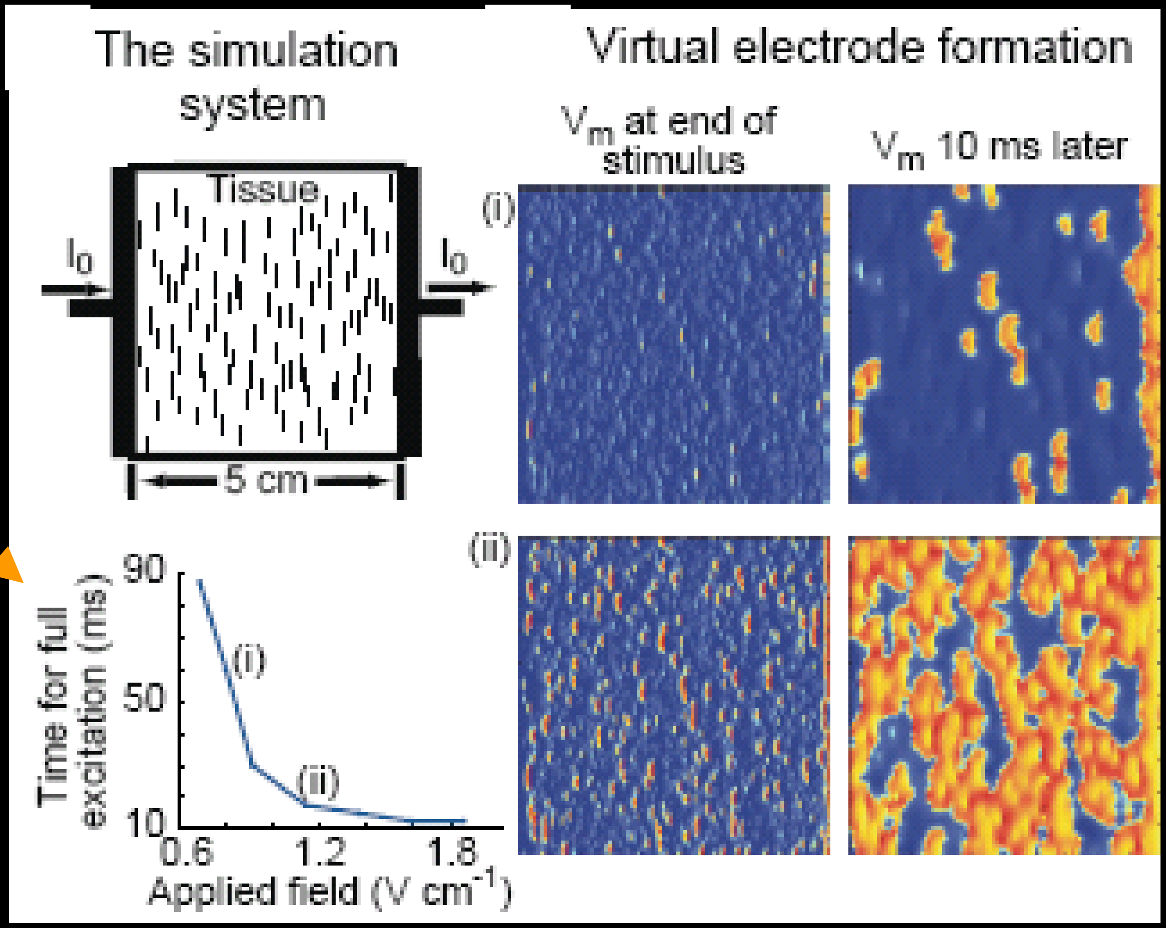

Defibrillation

Defibrillation then requires large energies to excite the whole tissue and terminate the arrhythmias.

Electrical cardioversion (requires >5V/cm)[1]

- External ~ 100J - 280J up to 360J (1000V, 30-45 A, 5ms)[3]
- Internal ~7J (350V, 4 A, 5ms)[2]

250V, 70mA, 1ms ~0.02J

1 Ideker RE, Zhou X, Knisley SB. Pacing Clin Electrophysiol 1995;18:512-525.
2 Santini et al. J Interv Card Electrophysiol 1999;3:45-51.
3 Koster et al. Am Heart J 2004;147:e20-e26.

A lower-energy alternative?

Objective

- Demonstrate that cardioversion can be achieved by a series of far-field low-energy pulses (~1.4V/cm) delivered at a frequency close to the dominant frequency of the arrhythmia.
- Internal ~7J (350V, 4 A) → (requires >5V/cm)
- This method is based on the idea of recruitment of virtual electrodes in cardiac tissue and global synchronization.

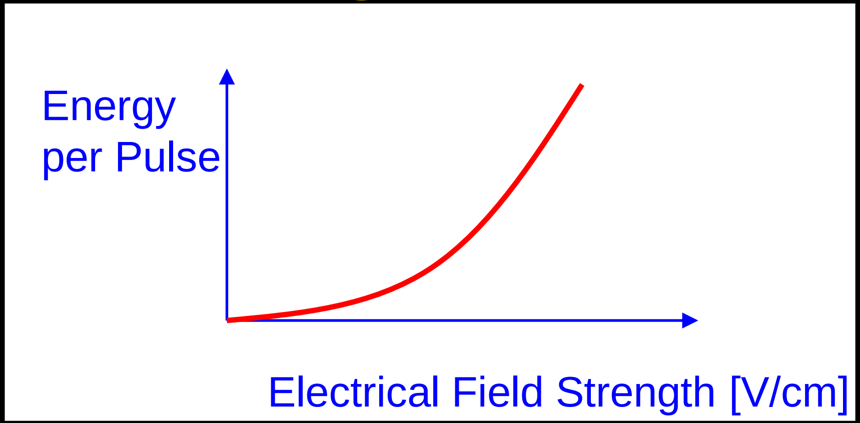

Defibrillation via Virtual Electrodes and Synchronization

Termination of spiral waves in simulated cardiac tissue by 4 low-energy shocks.

Bidomain (GMRES)
dx=.01cm, dt=.01ms
Zero-flux B.C.s, finite-volume
I_{ion}: Nygren et al. atrial cell model
Collagen ~.065cm

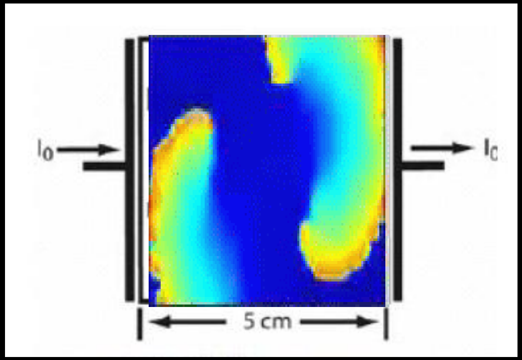

As the tissue synchronizes to the pacing period, more tissue gets activated simultaneously, and the reentries are terminated.

A new mechanism for defibrillation using up to 90% less energy than single shocks.

Defibrillation via Virtual Electrodes and Synchronization

Termination of spiral waves in simulated cardiac tissue by 4 low-energy shocks.

Bidomain (GMRES)
dx=.01cm, dt=.01ms
Zero-flux B.C.s, finite-volume
I_{ion}: Nygren et al. atrial cell model
Collagen ~.065cm

FTE

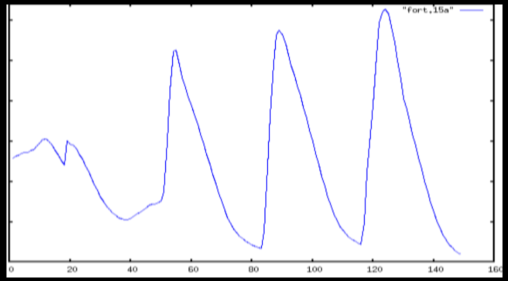

FTE/dt

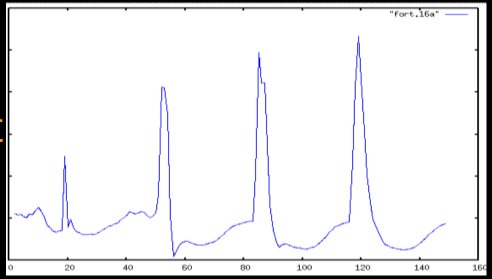

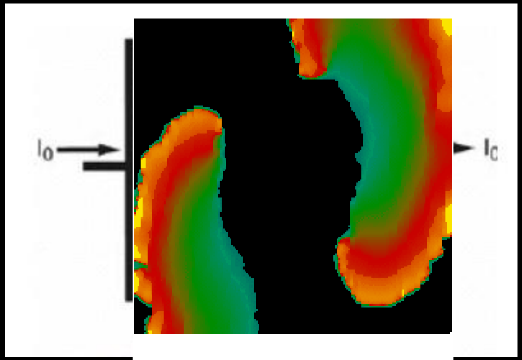

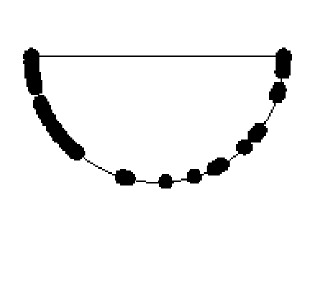

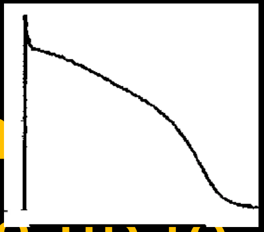

As the tissue synchronizes to the pacing period, more tissue gets activated simultaneously, and the reentries are terminated.

A new m
defibril ing up to
90% less energy than
single shocks.

Virtual Electrodes: Summary

- Larger heterogeneities are involved at lower field strengths.
- As more virtual electrodes are recruited, the time required to activate the entire tissue decreases (as more tissue is recruited).

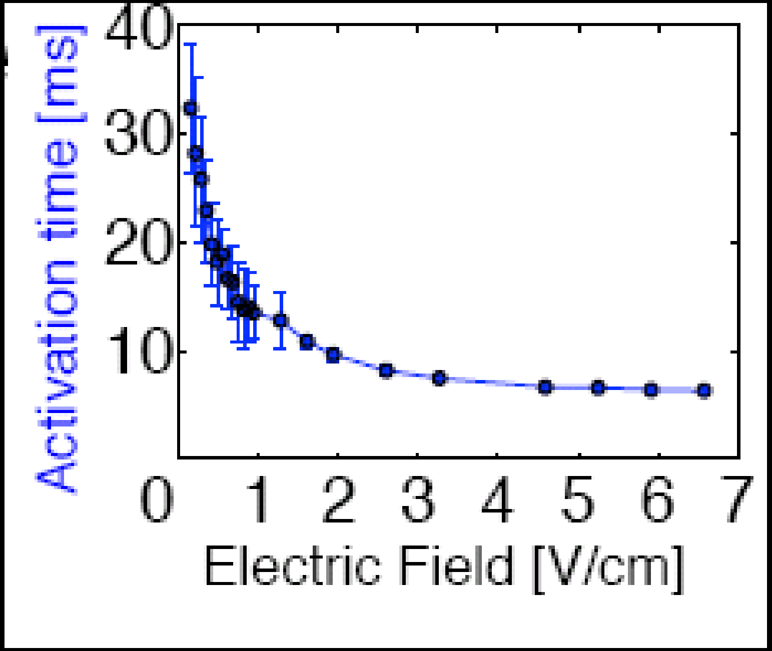

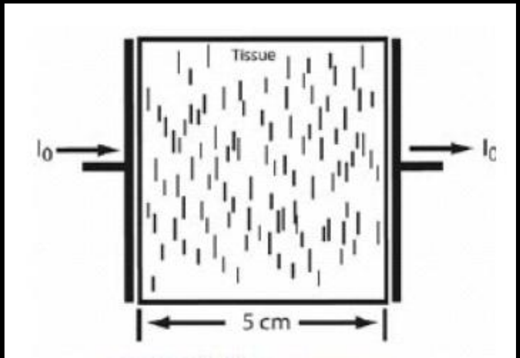

E=0.3V/cm

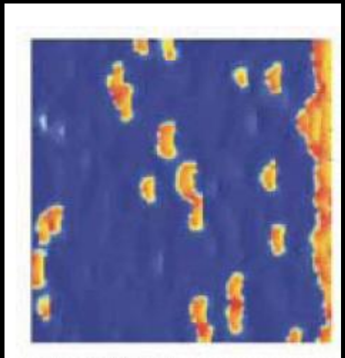

E=2.0 V/cm

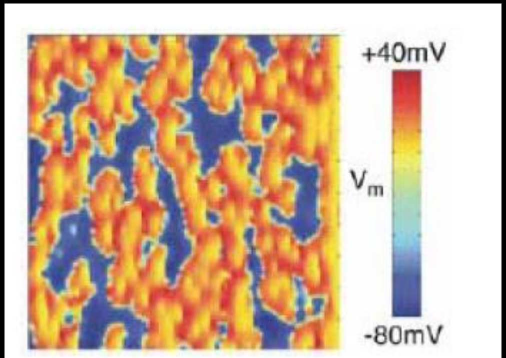

Virtual Electrode Formation: Experimental Confirmation

Point stimulus:
32 ms to activate

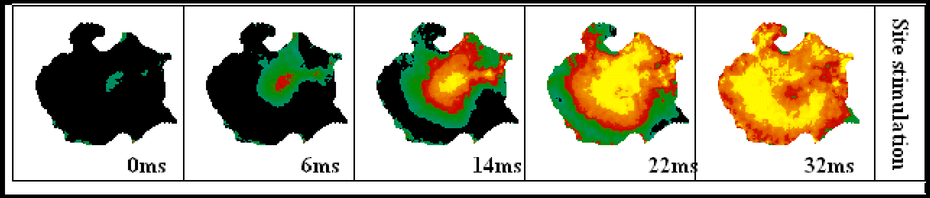

Fenton et al., Circulation, in press

Virtual Electrode Formation: Experimental Confirmation

Point stimulus:
32 ms to activate

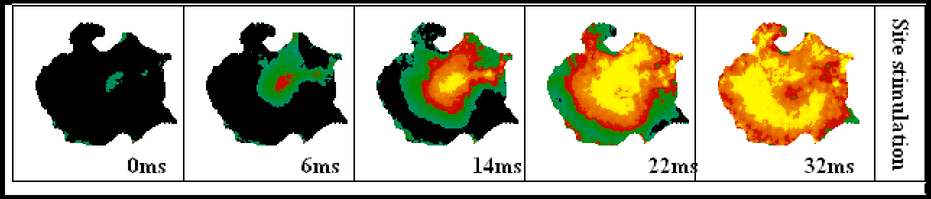

Electric field,
0.32 V/cm:
20 ms to activate

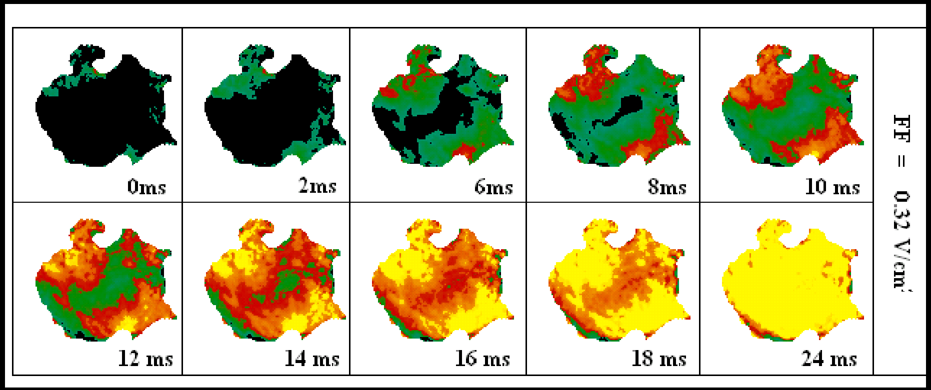

Fenton et al., Circulation, in press

Virtual Electrode Formation: Experimental Confirmation

Point stimulus:
32 ms to activate

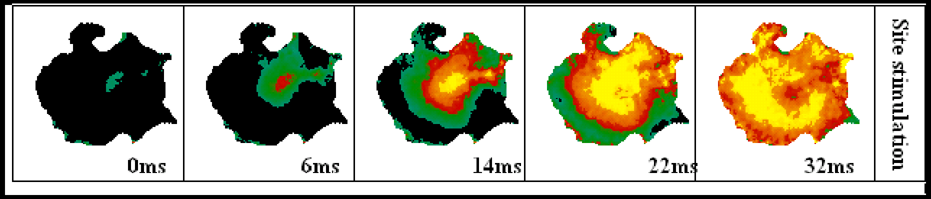

Electric field,
0.32 V/cm:
20 ms to activate

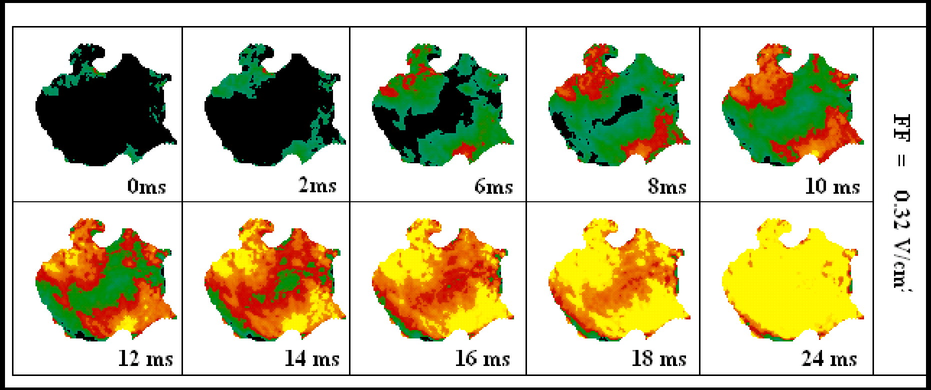

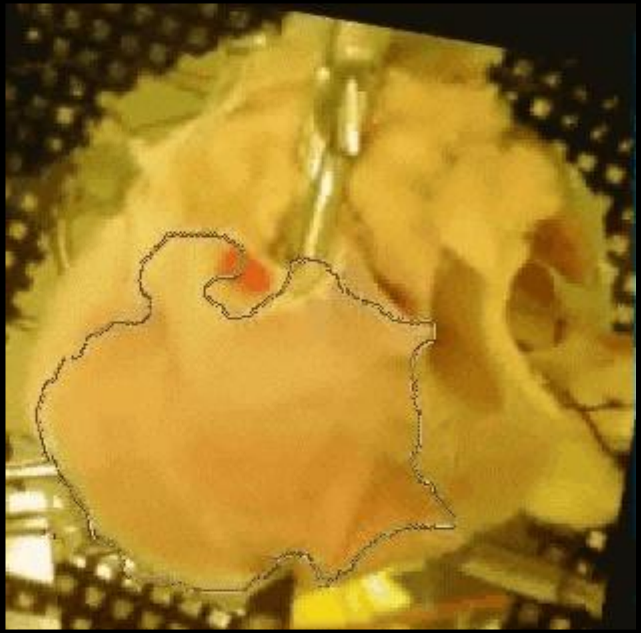

0.46 V/cm:
16 ms to activate

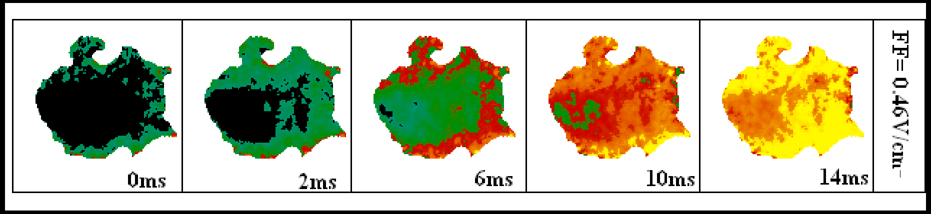

Fenton et al., Circulation, in press

Virtual Electrode Formation: Experimental Confirmation

Point stimulus:
32 ms to activate

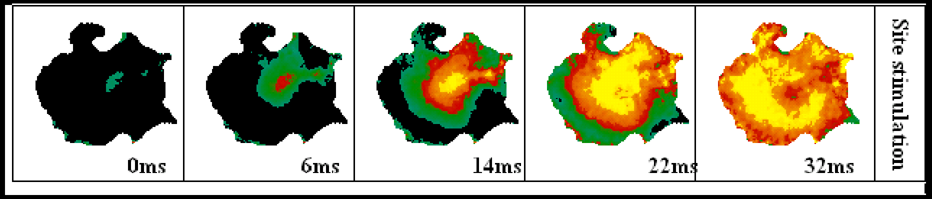

Electric field,
0.32 V/cm:
20 ms to activate

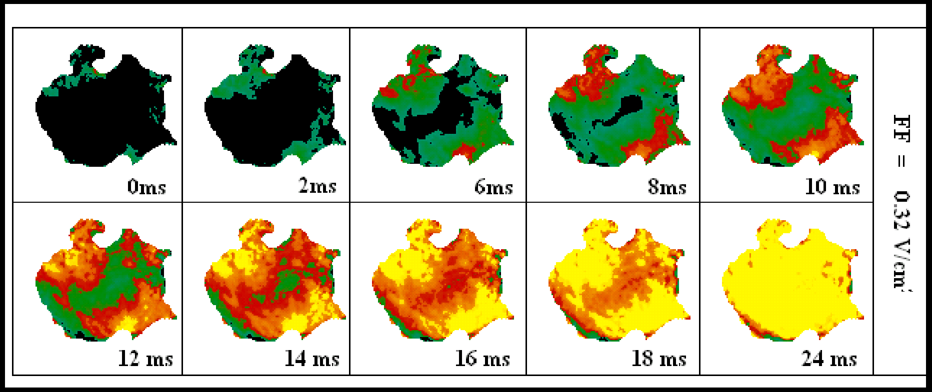

0.46 V/cm:
16 ms to activate

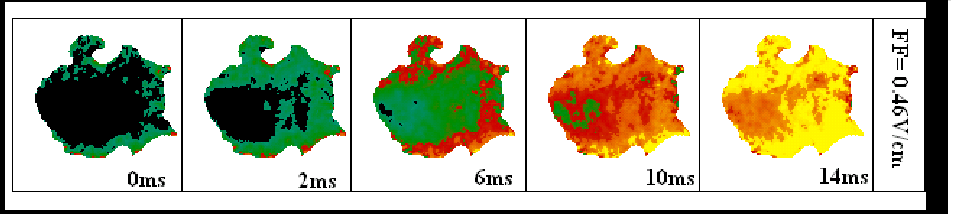

1.4 V/cm:
12 ms to activate

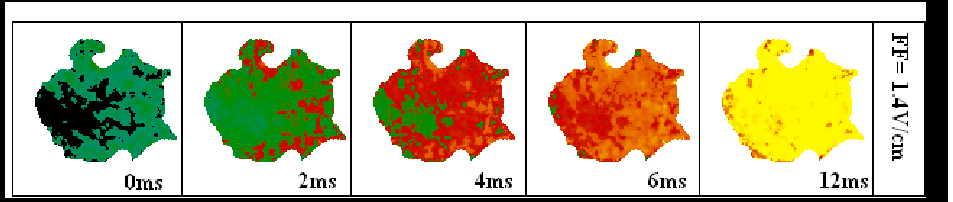

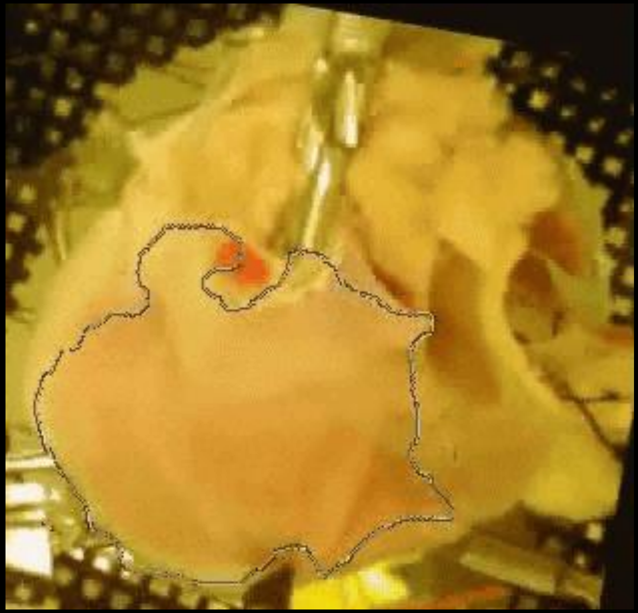

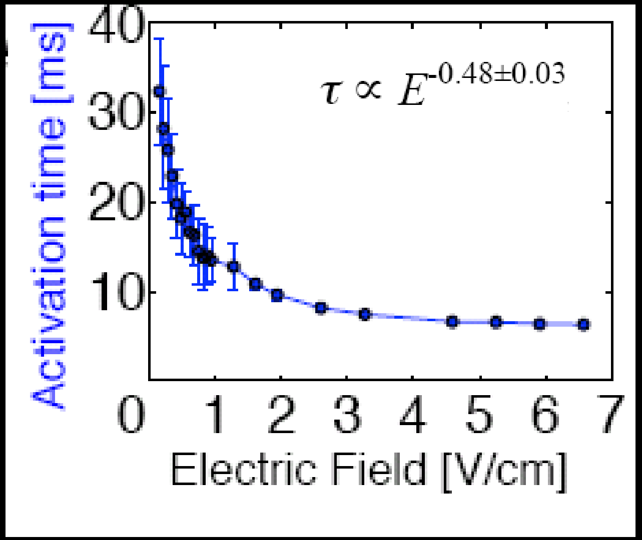

Average from 5 different experiments

Virtual Electrode Formation: Scaling law

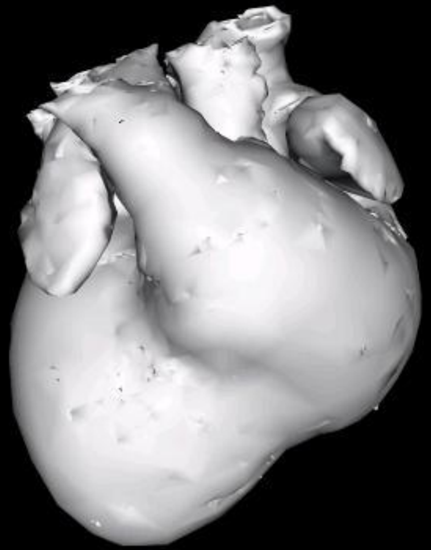

The change in membrane potential $e = V - V_{rest}$ around an obstacle by a small electric field is given by [1]

$$\nabla^2 e - \frac{e}{\lambda^2} = 0$$

With boundary conditions $\nabla(e + E \cdot \mathbf{r}) \cdot \mathbf{n} = 0$ at $r = R$

MRI digitized 4 canine hearts, 200-micron resolution

The minimum electric field E necessary to bring the voltage above threshold in 3D is given by

$$E = \frac{V_t - V_{rest}}{\lambda} \frac{1 + 2\alpha + 2\alpha^2}{1 + \alpha}$$

where $\alpha = \lambda / R$

For low electric fields $E \sim 1/R$

Conductivity discontinuities In the heart

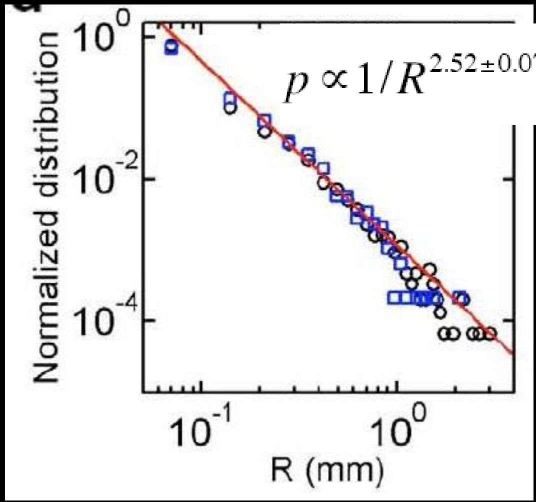

An activation from a SS propagating radially with constant velocity v will excite a volume $V = 4/3\,\pi(v\tau)^3$ at time t

For N obstacles uniformly distributed in tissue with $\rho = N/V$, the entire tissue will be excited in $\tau \approx (3/(4\pi\rho))^{1/3} / v$

The density of recruited obstacles is given by $\rho(E) = \int_{R_{\min}(E)}^{R_{\max}} p(R)\,\mathrm{d}R$

$\rho(E) \propto 1/R^{1.52} = E^{1.52 \pm 0.07}$

$\tau \propto E^{-0.51}$

[1] Pumir, A. and Krinsky, V., *J. Theor. Biol.* **199**, 311 (1999).

Examples of Low-energy Far-field Stimulation and Single High-energy Pulse Cardioversion

FF Failure E=0.9 V/cm

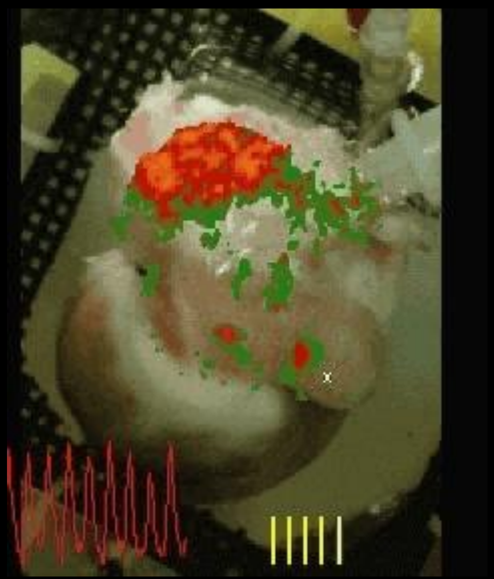

FF Success E=1.4 V/cm

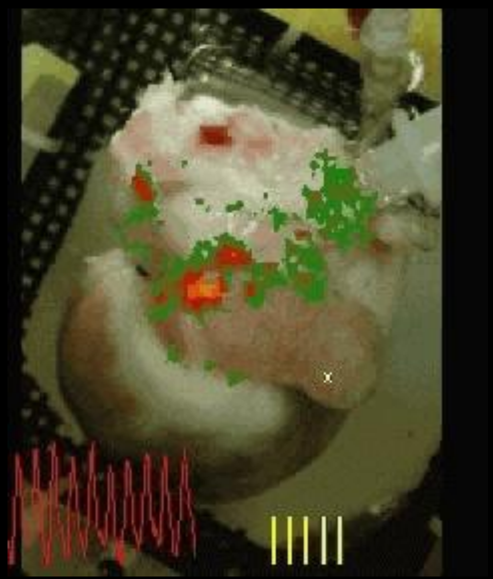

Cardioversion Failure E=4.0 V/cm

Cardioversion Success E=4.67 V/cm

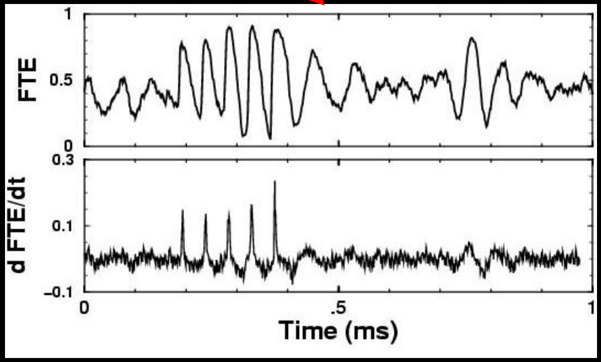

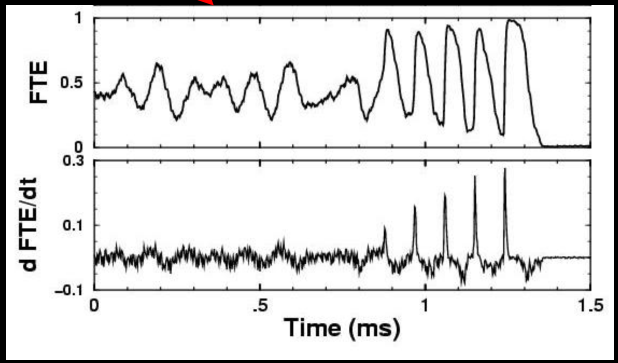

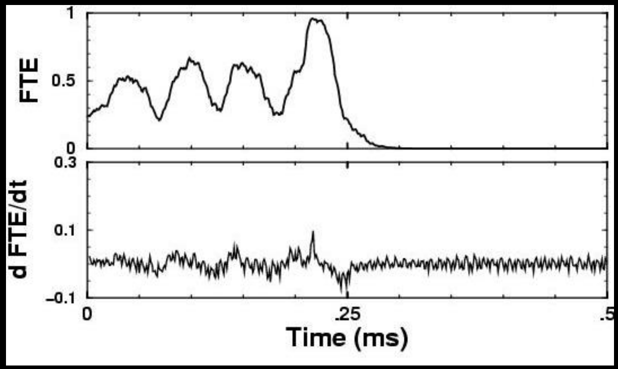

Examples of Low-energy Far-field Stimulation in Different *in Vitro* Preparations
Dominant periods 30 - 60 ms

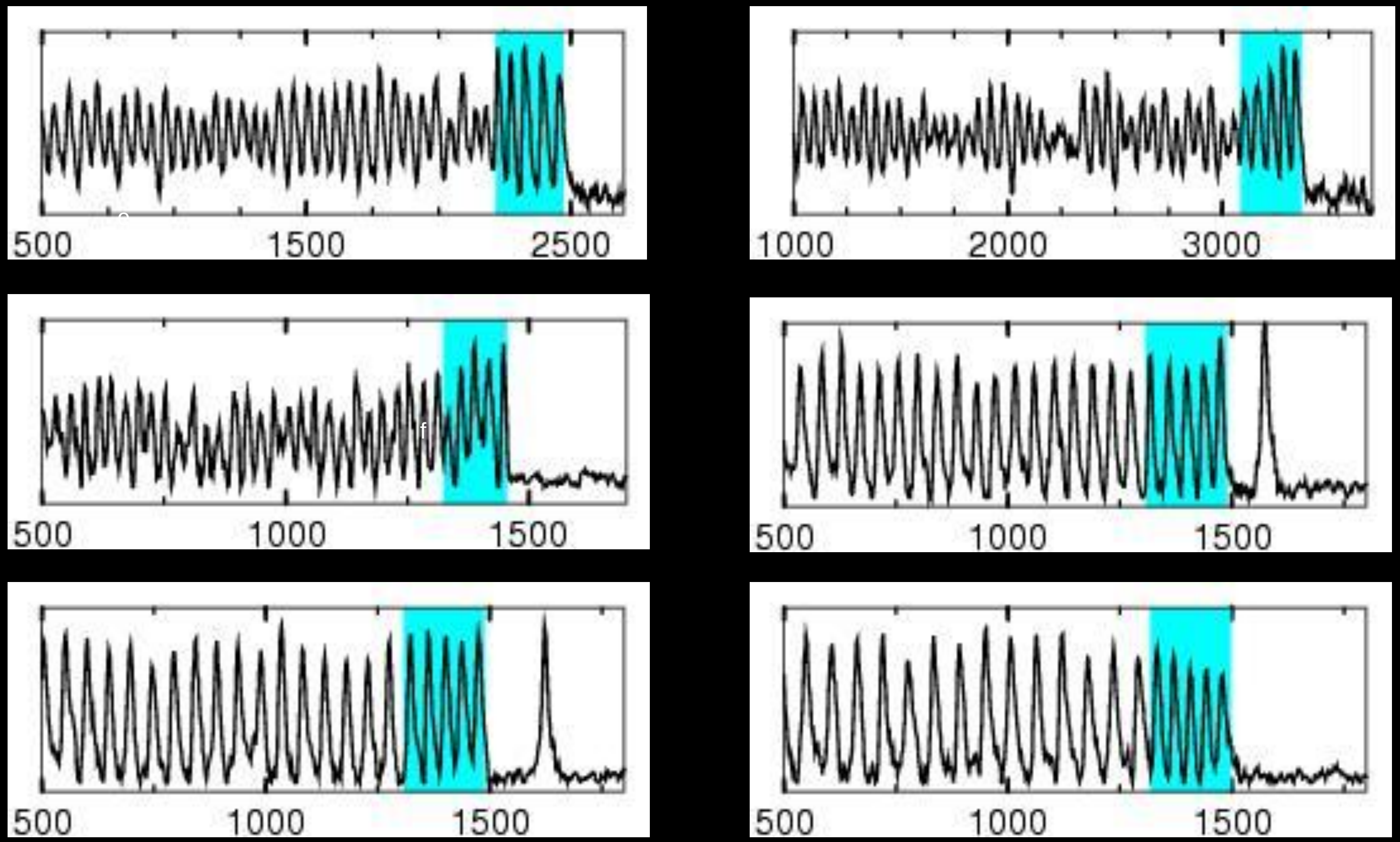

Success rate of 93 percent (69/74 trials in 8 canine atrial preparations).

FF-AFP reduces energy up to 90% in some examples.

Fenton et al.*Circulation 2009; 120, 467-476.*

Comparing *in vivo* and *in vitro*

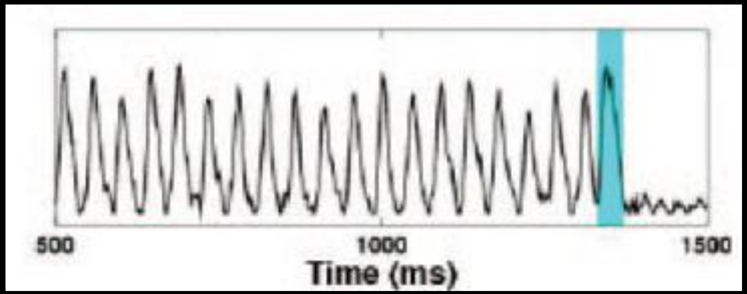

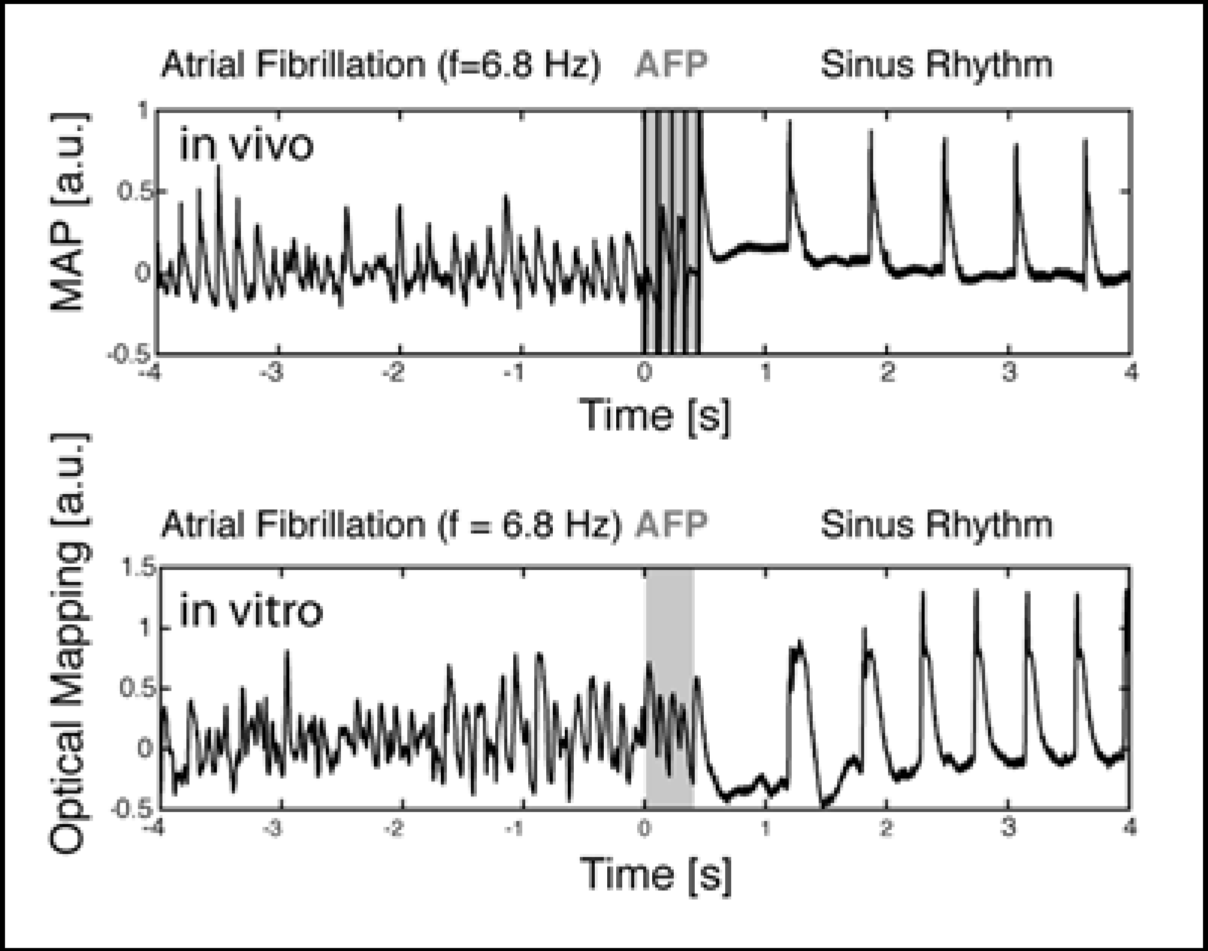

Comparing *in vivo* and *in vitro*

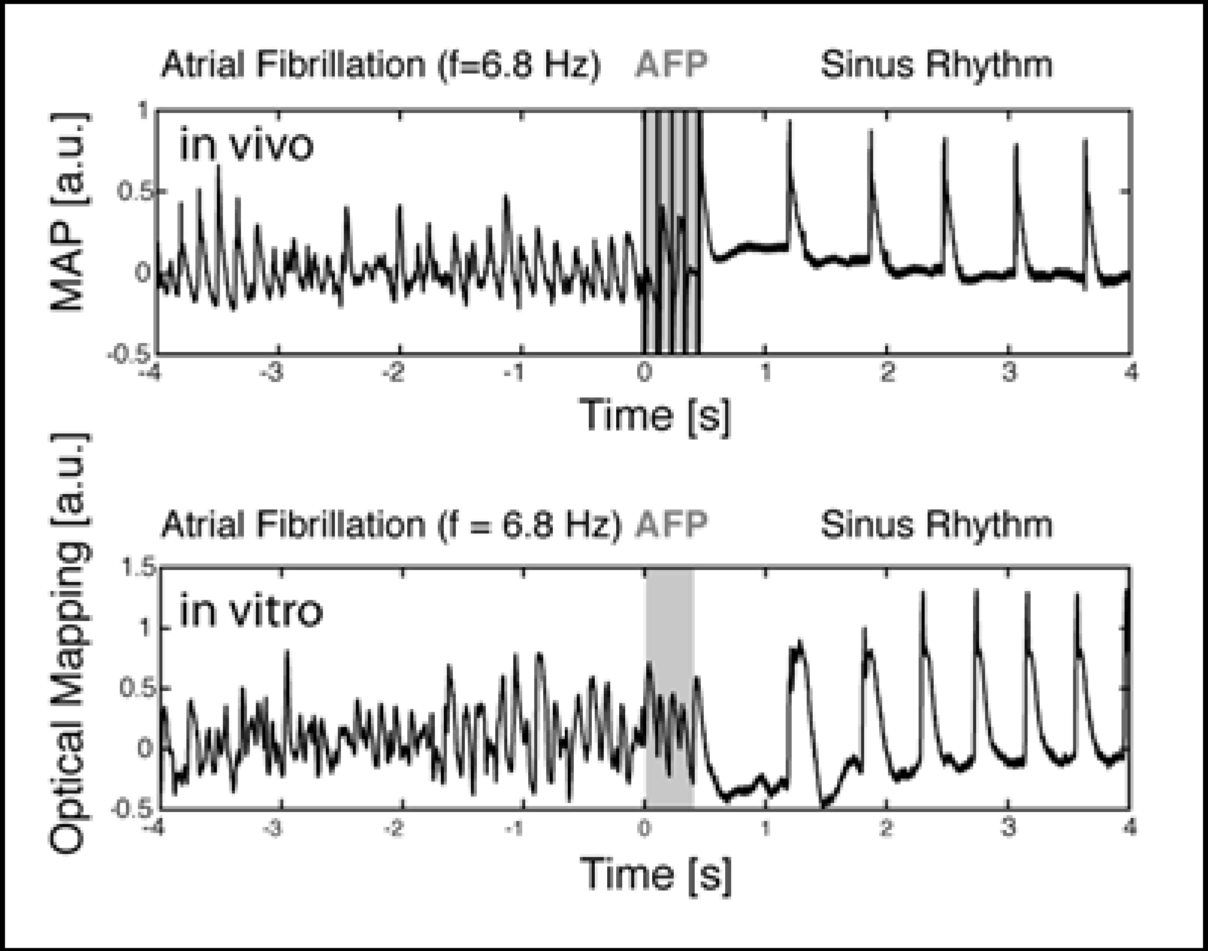

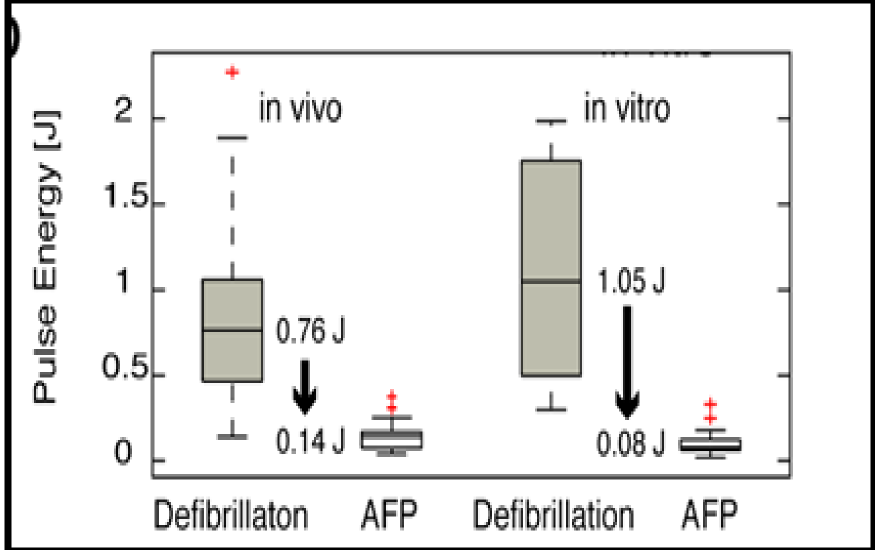

In vivo (N = 7): Cardioversion: 22 episodes, mean energy 0.89 ± 0.56 J.
AFP: 56 episodes, mean energy 0.14 ± 0.08 J.

In vitro (N = 5): Cardioversion: 39 episodes, mean energy 1.15 ± 0.58 J.
AFP: 46 episodes, mean energy 0.10 ± 0.07 J.

Take away message

- Heart function
- Many types of heart diseases (electrical just one of them)
- Chaos, complex systems and excitable media
- Fun with experiments
- Some basis on mathematical modeling of biological systems (MMBS)
- Some applications of MMBS and chaos dynamics.